8-10-2021

Separation of Short and Medium-Chain Fatty Acids Using Capillary Electrophoresis with Indirect Photometric Detection

Uyen Pham
upham4@student.gsu.edu

Follow this and additional works at: https://scholarworks.gsu.edu/chemistry_theses

Separation of Short and Medium-Chain Fatty Acids Using Capillary Electrophoresis with

Indirect Photometric Detection

by

Uyen Pham

Under the Direction of Shahab Shamsi, PhD

A Thesis Submitted in Partial Fulfillment of the Requirements for the Degree of

Master of Science

in the College of Arts and Sciences

Georgia State University

2021

ABSTRACT

Short and medium-chain fatty acids (SMCFA) are known as essential metabolites found in gut microbiota that function as modulators in the development and progression of many inflammatory conditions as well as in the regulation of cell metabolism. Currently, there are few simple and low-cost analytical methods available for the determination of SMCFA. This work focuses on the identification and measurement of SMCFA in rat feces utilizing capillary electrophoresis with indirect photometric detection (CE-IPD). In chapter 2, several parameters are optimized for maximum resolution, efficiency, and signal-to-noise ratio of FAs. The developed CE-IPD method is next validated in chapter 3 to quantify the FAs in healthy rat feces. Application to a pilot study on the influences of developmental stages (adult vs. adolescent) and various drug treatments on fecal SMCFA concentration in rats demonstrates the proposed CE-IPD method is an efficient tool for investigations on biological functions of SMCFA in clinical laboratories.

INDEX WORDS: Short and medium-chain fatty acids, Capillary electrophoresis, Indirect photometric detection, 5'-Adenosine monophosphate, Antibiotic, Cocaine

Separation of Short and Medium-Chain Fatty Acids Using Capillary Electrophoresis with

Indirect Photometric Detection

by

Uyen Pham

Committee Chair: Shahab Shamsi

Committee: Kathryn Grant

Samer Gozem

Electronic Version Approved:

Office of Graduate Services

College of Arts and Sciences

Georgia State University

July 2021

DEDICATION

This thesis work is dedicated to my parents, ba Cuu and me Linh, who have been a constant source of support and encouragement during the ups and downs of my graduate life. In one late night driving home from lab, I hit some big rocks on freeway. One of my car tires immediately went flat. It was lucky that I could safely slow down and pull over to the shoulder. It was midnight. It was raining. And my dad was driving to come pick me up in the middle of freeway. Moreover, I literally could not survive in long days and long nights at lab without everyday home-cooked meals made by my mom. This work is also dedicated to my best friend, Giang, who I believe "suffered" from my "nonstop" complaints about my difficulties and frustration with lab work. She cheered me up not just by saying "fighting" but sharing her thoughts on how she felt about what may come in life that I can totally relate to.

ACKNOWLEDGEMENTS

I would like to thank my advisor, Professor Shahab Shamsi, for his invaluable advice, support, and patience during the course of my MS degree. His expertise in pedagogy and chemistry guided me to become a researcher and bettered me as a chemist along the way. His contributions in revising this thesis also improved my writing skill, not only in this graduate program but extending to future career endeavors.

I would like to acknowledge my committee members, Dr. Kathryn Grant and Dr. Samer Gozem, who gave me inspiration to expand my chemistry interest to many different facets. Their dedication to students' success encouraged me to accomplish my work. I am grateful for their contributions in making me a better presenter, critical thinker, and writer.

I would like to thank my research collaborator, Dr. Kyle Frantz, and her group members, Gregory Suess, Elizabeth Sambor, Bonnie Williams, and Kevin Mesape. Without their contributions in experiments with rat feces, I would have not been able to complete my thesis project.

I would also like to thank my lab mates, Ferdoushi Akter, Vijay Patel, Mojibur Chawdhury, Kevin Sutherland, and Luis Alvarado, who offered me uncountable help and got me through the hardship when my experiments went wrong, when nothing worked out, and when I just needed someone to talk to.

TABLE OF CONTENTS

LIST OF TABLES

LIST OF FIGURES

1   LITERATURE REVIEW FOR SHORT AND MEDIUM-CHAIN FATTY ACIDS ANALYSIS BY VARIOUS CHROMATOGRAPHIC TECHNIQUES

1.1   Introduction and Scopes

1.1.1   Importance of Short and Medium-Chain Fatty Acids in Human Health

Gut microbiota is proposed to be related to human health via multiple activities such as modulating intestinal metabolism, regulating immune response, preventing pathogen invasion, boosting digestion, harvesting, and storing energy for colonocyte development [1]. The imbalance of gut microbiota increases the risk of various diseases like obesity, diabetes, inflammatory bowel, and cardiovascular diseases [2, 3]. These microbiota function in the form of short-chain fatty acids (SCFA), including acetic acid, propionic acid, butyric acid, isobutyric acid, valeric acid, and isovaleric acid as their end-products of anaerobic fermentation of carbohydrates, proteins, and amino acids. As the most abundant SCFA in the colon, acetic acid is a primary and significant energy source for tissues and the substrate of cholesterol synthesis [4]. On the other hand, propionic acid production is reported to inhibit cholesterol synthesis in hepatic tissue [5]. Thus, a balanced ratio of acetic acid and propionic acid can reduce the risk of cardiovascular disease. Furthermore, in-vitro studies have shown that both acetic acid and propionic acid significantly impact colonic blood flow, accelerating tissue oxygenation and transport of absorbed nutrients [6]. Besides, a significantly lower concentration of fecal acetic acid was reported in colorectal cancer patients than in controls [6]. Butyric acid is the most crucial SCFA as it has the most pronounced effect on the regulation of cell proliferation and differentiation. Various studies have been conducted on colonic adenocarcinoma cell lines, with results showing the cease in the growth of these cancer

cells in the presence of butyric acid [7, 8, 9]. Moreover, butyric acid induces apoptosis in colorectal tumor cells to a greater extent than acetic acid and propionic acid and at lower concentrations [6]. The other SCFA, including isobutyric acid, valeric acid, and isovaleric acid, produced at a lower concentration, are putrefactive fatty acids that imply underlying maldigestion and/or malabsorption, causing physiological disorders like hypochlorhydria and bacterial overgrowth in the small intestine [10].

Medium-chain fatty acids (MCFA) are obtained when medium-chain triglycerides are hydrolyzed in the gut. These acids are transported via the portal vein to the liver, where they are taken up by different tissues, which increases energy spent in muscle and fat, reducing obesity and preserving insulin action [11]. The production of MCFA also gives a high antibacterial effect as the anionic part of the molecule changes the pH of the digestive tract where microorganisms exist [12]. Van Immerseel et al. reported MCFA to possess more bactericidal power towards gram-positive and gram-negative bacteria than SCFA [13]. Notably, the authors demonstrated the addition of hexanoic acid led to a substantial decline in pathogen colonization in the gut. Besides, as reviewed by Lemarie et al., octanoic acid exhibits beneficial physiological outcomes on several diseases such as pancreatic insufficiency and fat malabsorption [14].

1.1.2 Scope of Review

Due to the importance of short and medium-chain fatty acids (SMCFA) in health promotion and disease prevention or treatment, various researches on SMCFA analysis have been investigated for more than three decades. Measurement of colonic fermentation via SMCFA is popularly based on indirect measures (e.g., feces, urine, or plasma) and various models (e.g., rodents, pigs, dogs, and humans). A brief literature

review on publications within ten years is implemented to overview recent scientific works on SMCFA determination in biological samples. Several database are utilized for literature search, including PubMed [15], SciFinder [16], Web of Science [17], and ScienceDirect [18]. Combination of keywords such as short-chain fatty acid, medium-chain fatty acid, feces, rat, and human, are input to the database to acquire relevant articles. The initial search results are further narrowed by adding the analytical method terms like gas chromatography (GC), high-performance liquid chromatography (HPLC), or capillary electrophoresis (CE). The current review focuses on three main chromatographic methods (GC, HPLC, and CE) with different detection techniques (e.g., flame ionization detection, mass spectrometry, direct or indirect UV detection) for SMCFA analysis. A comparison of the advantages and disadvantages of three methods for SMCFA analysis is outlined in Table 1.1.

1.2 Methods for SMCFA Analysis

1.2.1 Gas Chromatography

A classical analytical method for SMCFA separation and detection is GC coupled to a flame ionization detector (FID), widely applied to SMCFA determination in biological samples [2,4,19-21]. Comprising monocarboxylic head group and saturated hydrocarbon tail (2-12 carbon atoms), SMCFA possesses a certain degree of volatility, enabling them to be readily separated by GC. Many articles have reported a successful separation of SMCFA up to C7 (heptanoic acid) using GC-FID. For instance, Hu et al. [22] developed a direct GC method with HP-INNOWAX capillary column that satisfactorily separated SCFA from C2 to C5 with a lower limit of detection (LLOD) of 0.05-0.1 mmol/L and relative standard deviation (RSD) less than 5%. The method was

then applied to determine SCFA concentration in mouse colon feces of polysaccharide treated group compared to the control group. The GC column HP-INNOWAX was also employed by Tao et al. [23] for quantification of SCFA (C2-C5) in the colonic content of colitis mice. The LOD value was reported in a range of 0.097-0.274 ng/mL and the limit of quantitation (LOQ) 0.367-0.750 ng/mL. The method also provided low intraday and interday variations (1.32-3.33% and 2.97-4.69%, respectively). Besides, the matrix effect was examined to assure a reliable analytical result, which showed no significant suppression or enhancement for all six SCFAs.

In another study, Zhao et al. [24] proposed a GC method using a DB-FFAP capillary column, which features high polarity for analysis of volatile FAs. Quantitation of SMCFA (C2-C6) was achieved in rat feces with LOD value of 0.0868-0.393 µg/mL and LOQ 0.261-1.18 µg/mL with intraday and interday precision less than 2.54% and 4.33%, respectively. The stability of SMCFA was also tested to be good over 12 hr analysis at room temperature. Moreover, to prevent contamination of the GC column, a glass liner stoppered with a glass wool plug in the middle of the liner was included in the GC system. In a publication by Wang et al. [25], DB-FFAP capillary column was also utilized in determining SMCFA from C2 to C7 in intestinal bacteria from rat donors. The authors adopted different oven temperature programming, e.g., from 90°C to 200°C compared to the abovementioned Zhao et al.'s method (50°C to 240°C). The percent recovery of SMCFA (C2-C7) was improved and obtained at a narrower range, i.e., 98.0-102.2% compared to 92.8-104.1% by Zhao and coworkers. Most recently, Kim et al. [26] introduced solid phase extraction sample cleanup before GC-FID analysis of SCFA

(C2-C5) in a cultured microbial sample, which substantially reduced baseline noise and successfully eliminated interfering peaks from the matrix.

Despite the widespread use, FID generally requires high temperature (200-250°C) to operate the separation, which creates a high risk of destroying the sample, consequently requiring additional air and hydrogen to compromise the issue. Mass spectrometry (MS) is an alternative detector coupled with GC that can provide thermal stability for FA analysis in which derivatization is required. Zheng et al. [27] reported using propyl chloroformate (PCF) as a derivatization reagent for determining SMCFA (C2-C7) in feces from rats and humans. The derivatization method was optimized to one-step derivatization of 100 μL PCF in reaction system of water, propanol, and pyridine (v/v/v = 8:3:2) at pH 8. Next, the derivatized products were extracted with hexane twice to maximize the extraction efficiency, which resulted in over 95% efficiency of SMCFA propyl esters. The RSD values of peak intensities for intraday and interday precision were less than 10%. The stability for derivatized SMCFA was also studied, showing RSD lower than 20% for peak areas for four days at room temperature and seven days when stored at -20°C. The LOD values were reported ranging from 20 to 1000 pg. Unfortunately, LODs of acetic acid and propionic acid were not calculated because these two compounds were detected in a blank water sample introduced by the impurity of derivatization solvent.

Pentafluorobenzyl bromide (PFBBr) is another derivatization reagent that has been employed for GC-MS quantification of SCFA in biological samples [28-30]. For example, He et al. [28] optimized PFBBr derivatization in acetone/ water solvent (v/v = 2:1) at pH 7 in 90 min reaction to derivatize C1 to C5 FA., except for C1 (formic acid).

However, these derivatizing conditions did not significantly lower the intensity of the PFBBr derivative of C1. In addition, the study on derivatization reaction temperature indicated a direct relationship between the intensity of PFBBr derivatized SCFA and temperature, resulting in the highest intensity at 80˚C. However, protein denaturation occurs at 80˚C, consequently, denatured protein could disturb the extraction efficiency of PFBBr derivatives. Thus, 60˚C was selected as the optimal derivatization temperature. Besides, the authors proposed a GC-MS method that included two columns, DB-225ms (polar) and DB-5ms (non-polar), which are hyphenated together by a column connector, to obtain the best resolution of target compounds without interference from solvent peaks. The exclusive achievement of the work mentioned above was claimed to detect and quantify formic acid that had not been reported before. Another derivatization reagent used in GC-MS analysis is N,O-bis(trimethyl-silyl)-trifluoroacetamide (BSTFA) [31]. It is worth mentioning that due to its sensitivity to moisture, this above reagent is not specified for SCFA. However, the issue was successfully resolved with sodium sulfate dehydration pretreatment. The method provided high repeatability of retention time and peak area (RSD < 2.18%) and low LOD (0.064-0.067 μM). Furthermore, the study on derivatization efficiency indicated at least 2 hr reaction at 37˚C required to reach the highest value. This time delay makes longer analysis time.

Recently, several GC-MS methods without derivatization are developed to simplify sample preparation and avoid time-consuming derivatization reaction. For instance, Lottie et al. [32] established a fast and cost-effective GC-MS method to quantify FA up to C16 in human biofluids. In the above method, solid-liquid extraction

(SLE) was performed in phosphate buffer saline, followed by acidification in H_3PO_4, and liquid-liquid extraction (LLE) in methyl tert-butyl ether (MTBE). However, the percent recovery was obtained in a more extensive range (75.4-124.4%) than the data obtained from the derivatization of FAs by GC-MS methods reported by Zheng et al. [27] and Zhang et al. [31]. Both above-mentioned methods reported recovery in the range of 81.1-118.8% and 81.3-128.4%, respectively. On the other hand, Hsu et al. [33] indicated MTBE solvent used in LLE resulted in poor recovery for acetic acid. Therefore, the authors suggested butanol as a compromising extraction solvent for good recoveries of all target SCFA. Han et al. [34] proposed an underivatized GC-MS method that provided relatively high precision (<5%) and good recovery (88.8-105.0%). Nonetheless, a multi-step sample pretreatment procedure was required, including lyophilization at -80°C, <10 Pa, and in 3.5 hr, followed by SLE with water/H_2SO_4/ether (v/v/v = 0.8:0.2:1), LLE with diethyl ether, centrifugation, and acidification with $CaCl_2$. Fiori et al. [35] demonstrated another cleanup method, i.e., headspace-solid phase microextraction, applicable to direct sampling of SCFA with sufficient sensitivity (LOQ 0.011-0.23 µmol/g), good precision (<11%), and recovery (79-110%).

1.2.2 *High-performance Liquid Chromatography*

One of the alternative methods for SMCFA analysis in biological samples is HPLC. Similar to GC, sample pretreatment (derivatization), column, and detector selection must be evaluated and optimized for a successful SMCFA analysis. Very few HPLC methods using UV detection without derivatization is reported in the literature in the past ten years. Nonetheless, a direct HPLC-UV method was presented by Baere and coauthors in 2013 for the quantitative determination of four SCFAs (C1-C4) and

lactic acid in fecal bacterial culture samples [36]. Multi-step sample pretreatment was carefully implemented to assure a good extraction and purity of SCFA. Detection was performed only at a short non-selective UV wavelength (210 nm) due to non-UV-absorbance of SCFA. The separation was conducted on Hypersil Gold endcapped C18 column providing LOD ranging from 0.13 to 0.33 mM and LOQ 0.5 to 1.0 mM with precision less than 16%.

Gardana and coauthors, in 2017, reported ultrahigh performance liquid chromatography coupled to orbitrap (high resolution) mass spectrometry (UHPLCHR-MS) to simultaneously separate, detect and quantify SCFA (C2-C5) together with lactic, pyruvic, and succinic acids in human fecal samples [37]. Despite the partial separation of succinic acid, pyruvic acid, and acetic acid, as well as only near baseline separation of butyric acid/ isobutyric acid, the UHPLCHR-MS method showed sufficient precision (<10%), recovery (83-105%), LOD, and LOQ in the range of 0.04-0.23 and 0.2-0.5 µg/mL, respectively. Furthermore, a study on method comparison among UHPLCHR-MS, GC-FID, and HPLC-UV demonstrated a good correlation in the amounts of SCFA determined by UHPLCHR-MS and GC-FID, but a disagreement with the result from the HPLC-UV method. The main reason was the lack of chromophores in the traditional HPLC-UV method, leading to lower accuracy in determining the actual amount of SCFA in fecal samples.

Besides the direct HPLC method, derivatization seems to be more favorable as it increases the sensitivity and selectivity of the analytes. Various derivatization reagents has been used for SMCFA analysis by HPLC-MS/MS such as 3-nitrophenylhydrazine [38], aniline [39], 2-bromoacetophenone [40], 2-picolylamine [41], O-

benzylhydroxylamine [42], and 4-acetamido-7-mercapto-2,1,3-benzoxadiazole [43]. In

addition to common sample cleanups like SLE and LLE, Nagatomo et al. [41] also

applied the QuEChERS method, which is highly suitable to biological samples, for

recovery enhancement. Moreover, the LOD and LOQ obtained from derivatization

before HPLC-MS analysis was reported as low as in the fmol range [38, 42], nM [39,

41], or ng/mL [40, 43], indicating excellent method sensitivity.

1.2.3 Capillary Electrophoresis

Another alternative analytical method that advantageously offers short analysis

time, lower sample and reagent consumption, as well as simple sample preparation, is

CE. Many reports have been published on FA analysis in food, beverages, and

environmental samples using CE, but not widely on SMCFA in biological samples. In

particular, over the past ten years, only three papers proposed the CE method to

determine SCFA (C2-C4) in fecal samples [44-46]. Due to non UV absorbing of SCFA,

CE detection is conducted with a chromophore in background electrolyte (BGE), called

indirect photometric detection (IPD) reagent. Two papers [44, 45] employed benzoic

acid as an IPD reagent. In the first paper by Marques et al. [44], three SCFAs, acetic,

propionic, and butyric acids, were successfully separated and detected in mice feces

within 10 min. There was no derivatization as well as multi-step organic solvent

extractions needed. The method showed good precision (<10%) and recovery (74.1-

109.8%). The LOD and LOQ for SCFA were reported in the range of 0.03-0.13 and

0.09-0.43 mM, respectively. In the second paper by Hodek et al. [45], SCFA from C2 to

C4 FAs, including isomer of C4-FA, were satisfactorily resolved in 10 min. Still, there

was partial coelution of matrix peaks from FAs peaks in fecal samples. The LOQ was

reported in two units (concentration and mass) considering the form of the sample, i.e.,

8-10 µmol/L of injected extract and 5.9-7.0 µg/g of the original sample. The method

demonstrated acceptable precision (<14%) and recovery (90.4-114.9%). The third

paper by Lemay et al. [46], published in early 2021, utilized three anionic chromophores

in the BGE, including 1,3(6,7)-naphthalenetrisulfonate, 1,5-naphthalenedisulfonic acid,

and sodium chromate, for fecal SCFA (C2-C4) determination in pediatric inflammatory

bowel disease patients. The LOD and LOQ were reported in the range of 1.2-3.6 and

4.0-12 µM, respectively, with precision less than 13% but quite a low recovery (83-

85%). In addition, the authors did not attempt to resolve BA and IBA with an explanation

of the extremely low natural abundance of IBA in fecal extract previously reported in the

literature. Besides, up to date, CE coupled with MS has not been applied to the

determination of SMCFA in fecal samples yet, even though this combination might

provide higher separation efficiency and sensitivity.

1.3   Indirect Photometric Detection in Capillary Electrophoresis

1.3.1   Concept and Principle

The IPD in CE is a detection mode where a UV transparent species becomes

detectable by adding the same charge but a UV absorbing species at a relatively lower

concentration (e.g., 2-10 mM) range than the BGE in the separation capillary. When

the migrating non UV absorbing species reaches the detection window, a displacement

of the UV absorbing species in the BGE is created, leading to a decrease in the

background absorbance. The electropherogram will result in a negative peak, indicating

a detection of the UV inactive species. For a convenient visualization and peak

quantitation, the negative peak can be inverted to positive by switching the detection and reference wavelengths.

The basic principle by which the concentration limit of detection (C_{LOD}) for a non-absorbing analyte is determined is formulated by Macka and Haddad [47] as below:

$$C_{LOD} = \frac{C_M}{DR \times TR} = \frac{N_{BL}}{TR \times \varepsilon l} \qquad (1)$$

where C_M is the concentration of the UV absorbing species, DR is the dynamic reserve (i.e., the ratio of the background absorbance to the noise), TR is the transfer ratio (the number of moles of the IPD reagent displaced by one mole of the analyte), N_{BL} is the baseline noise, ε is the molar absorptivity of the IPD reagent, and l is the pathlength of the detection cell. According to equation (1), C_{LOD} can be improved by reducing C_M or increasing DR. However, DR is directly related to C_M, so decreasing the IPD reagent concentration will also decrease DR, making almost no improvement in the detection limit. Consequently, minimizing C_{LOD} often involves maximizing DR by either reducing the background noise or increasing the background absorbance of the IPD reagent. The values of C_{LOD} for IPD around $10^{-4} - 10^{-5}$ M are routinely achieved in CE is combined with IPD [48].

Furthermore, C_{LOD} in equation (1) is influenced by TR in an inverse relationship. In other words, a higher value of TR, a larger analyte peak area, a better C_{LOD}. One might expect that the displacement of the IPD reagent by migrating analyte ion would occur on an equivalent-per-equivalent basis so that a TR between a singly charged analyte and a singly charged IPD co-ion would be unity. Consequently, peak areas for analyte ions of the same charge and concentration would be similar, allowing one universal calibration. However, Ackermans et al. [49] discovered that the ionic species'

peak areas and effective mobilities for an equimolar sample composition experienced a non-linear relationship. The results were explained based on Kohlrausch's regulating function (ω) as follow:

$$\omega = \frac{C_i Z_i}{\mu_i} = \text{constant} \tag{2}$$

C_i, Z_i, μ_i represent the ionic concentration, absolute values of the charge, and absolute values of the effective mobilities of all ionic species, respectively.

At the beginning of the separation, a specific volume element of the capillary is filled with a UV absorbing ion A (IPD reagent) at a concentration C_A and a non UV absorbing counterion C. When the analyte ion B is injected, voltage is applied. As a result, the analyte ion B migrates through this volume element, containing both ions A and B for a while, and then the actual situation is restored. The analyte ion migration was demonstrated by Ackermans et al. as follow:

$$C_A^C = C_A^S + C_B^S k_B \tag{3}$$

The superscripts C and S in equation (3) refer to the concentrations of the IPD electrolyte zone and the solute zone, respectively. As stated in the review by Shamsi [48], equation (3) can be verified from Kohlrausch theory according to equation (4):

$$k_B = TR = \frac{Z_B\,\mu_A\,(\mu_B + \mu_C)}{Z_A\,\mu_B\,(\mu_A + \mu_C)} \tag{4}$$

where k_B is referred to as the TR (also called the response factor); Z_A and Z_B represent absolute charges on the IPD co-ion A and analyte ion B, respectively; μ_A, μ_B, and μ_C refer to the effective electrophoretic mobility of the IPD co-ion A, analyte ion B, and the non-absorbing counterion C, respectively.

The absorbances of the IPD ion (A^C) and the sample ion (A^S) can be written in accordance with Beer's law as follows::

$$A^C = \varepsilon_A\, C_A^C\, l \qquad\qquad (5)$$

$$A^S = \varepsilon_A\, C_A^S\, l + \varepsilon_B\, C_B^S\, l \qquad\qquad (6)$$

From equation (3), the UV signal generated as a change in background absorbance (ΔA) will be:

$$\Delta A = A^C - A^S = C_B^S\, l\,(\varepsilon_A k_B - \varepsilon_B) \qquad\qquad (7)$$

For non UV absorbing analyte ion, $\varepsilon_B = 0$. Substituting for the k_B (aka TR) from equation (4), equation (8) was derived:

$$\Delta A = C_B^S\, l\, \varepsilon_A\, \frac{Z_B\, \mu_A\,(\mu_B + \mu_C)}{Z_A\, \mu_B\,(\mu_A + \mu_C)} \qquad\qquad (8)$$

As indicated in equation (8), the value of ΔA (i.e., detection sensitivity) in a solute zone is proportional to the value of TR, the ratio of the charge of the solute, and the light-absorbing electrolyte ion, as well as the concentration of the solute ion. Therefore, the large value of TR will provide high detection sensitivity, or in other words, better LOD.

1.3.2 Factors in Detection Sensibility

Sensitivity in IPD is governed by many factors that should be carefully investigated in method development for a specific group of analyte ion separations in CE. First, a couple of characteristics such as molar absorptivity and mobility should be considered in selecting an IPD reagent for the separation. Second, the concentration of the IPD reagent and its pH need to be optimized due to their influences on the charge displacement. Third, the type and concentration of the non-absorbing BGE also play a role in separation sensitivity as competitive displacement might occur between non-absorbing ion and IPD ion. Finally, the other factors like detection wavelength, background noise, and absorption pathlength also impact sensitivity in IPD.

1.3.2.1 Molar Absorptivity of IPD Reagent

When choosing an IPD reagent for a specific separation, the first factor is the molar absorptivity (ε) of the IPD reagent. According to equation (1), the high value of ε provides high DR, meaning a low concentration of IPD reagent could be utilized, overall resulting in a low value for LOD. Nevertheless, the benefit of high ε is only achieved in full when the IPD ion mobility matches the electrophoretic mobility of the analyte ion. As comprehensively reviewed by Shamsi [48], many publications reported the IPD optimization based on the ε. For instance, sorbate (high ε) provided 50-times improvement in LOD compared to benzoate (low ε), or in comparison among ribonucleotide electrolytes (adenosine, cytidine, guanosine, and uridine monophosphate – AMP, CMP, GMP, and UMP) as IPD reagent, AMP was found to provide the best LOD because if its high ε and closest mobility match to the analytes.

1.3.2.2 Mobility of IPD Reagent

As mentioned earlier, the matching in mobility between IPD ion and analyte ion is critical to achieving an optimum sensitivity in IPD. Notably, a degree of mobility matching is illustrated in electropherogram via peak shapes of the analytes. Electrolyte ion with a slower mobility than the analyte will cause a non-Gaussian distribution of migrating zone where there is a diffusion at the front. The rear becomes sharp, resulting in a fronting peak. On the contrary, electrolyte ion with faster mobility than the analyte exhibits a tailing peak. A symmetrical peak is only obtained when the mobility of the electrolyte ion and the analyte ion is similar. A straightforward relationship between mobility match and peak shape is demonstrated by Jones and Jandik [50], where three IPD electrolytes: chromate (high mobility), phthalate (intermediate mobility), and p-

hydroxybenzoate (low mobility) were studied. Figure 1.1 shows the comparison of peak symmetry of anions using these three IPD electrolytes. It is seen that chromate has mobility close to inorganic anions (peaks 1 and 2), phthalate has mobility comparable to the carboxylates (peaks 3-5), and p-hydroxybenzoate has mobility close to short-chain linear alkanesulfonates (peaks 6 and 7).

1.3.2.3 Concentration of IPD Reagent

Another crucial factor in IPD sensitivity is the concentration of the IPD reagent due to two main reasons. First, the ratio of the light-absorbing electrolyte concentration to analyte concentration is directly related to peak efficiency and resolution. In particular, the ratio of the conductivities of the analyte and the electrolyte controls the peak shape. Second, the concentration of the IPD reagent should give a background absorbance within the linear range of the detector, whereas background noise and joule heating must remain low. It is reported that the concentration of most of the IPD electrolytes is used in the range of 1-10 mM [48].

1.3.2.4 pH of IPD Reagent

In CE separation, pH affects the ionization of all species present in BGE. Significantly, the pH of the light-absorbing electrolyte should be such that the contribution of non-UV-absorbing H^+ and OH^- ions is minimized during the charge displacement process. For instance, at very high pH (>12), which is required for ionization of weakly acidic compounds (e.g., carbohydrates), the concentration of OH^- ions is no longer negligible relative to the concentration of IPD electrolyte. Consequently, TR is reduced, causing a decrease in IPD sensitivity.

1.3.2.5 Type and Concentration of Non-absorbing Buffer

Although IPD reagent can be used as buffer itself, some disadvantages are found, such as the pH buffering range is limited to narrow regions around p*Ka* of the IPD reagent, partially ionized IPD co-ions that limits its applicability to various analytes, and buffer capacity is limited to the concentration of the IPD reagent. Thus, non-absorbing co-anionic buffers such as borate, acetate, phosphate, and carbonate, or non-absorbing countercations such as Tris and triethanolamine, is more favored in CE-IPD separation [48]. Besides, the concentration of the non-absorbing buffer should be optimized because a too high concentration of non-absorbing buffer may cause a decrease in *S/N* due to dilution of the light-absorbing ion zone. Furthermore, the presence of the non-absorbing co-ion can induce a system peak that potentially interferes with analytes of interest [48].

1.3.2.6 Other Factors

The choice of an appropriate detection wavelength is another approach to optimize the sensitivity. Because most inorganic anions and cations have no UV absorbance at any wavelength, the detection wavelength can be chosen to favor strong UV absorbance of IPD reagents. Wavelengths used in IPD are typically in the range of 185-365 nm [48]. In addition, minimizing optical background noise is generally based on light-emitting diodes that can provide good baseline stability and reduced noise level up to one order of magnitude [48]. However, the IPD reagents must absorb light in the visible region to use these diodes. Two major problems are concerned. First, chromophores having intense absorption in the visible region are large organic molecules with lower mobilities that do not match those of the analytes (e.g., high-

mobility inorganic anions), and second, the adsorptive interactions of such molecules

with the capillary cause baseline fluctuation [48]. Hence, employing light-emitting diodes

in IPD is not preferable to the use of UV lamp sources. Besides, extended absorption

pathlength is also a desirable factor for sensitive detection as it increases background

absorbance. An extended pathlength from 75 µm to 300 µm at the detection window

("bubble cell") was reported to increase the IPD signal by a factor of approximately two

without increasing joule heating [51].
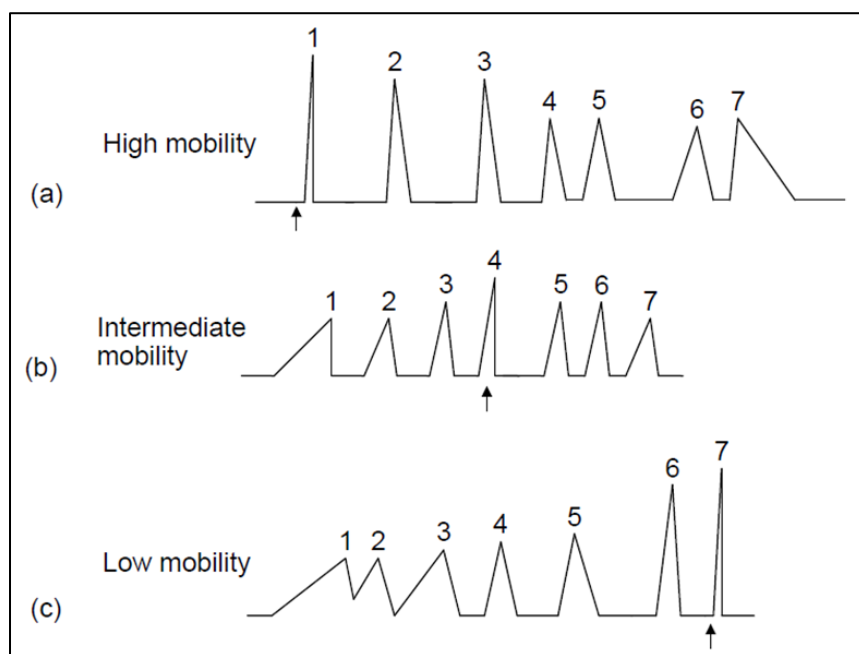
Figure 1.1 Comparison of the peak symmetry for high-mobility (a), intermediate-mobility (b), and low-mobility (c) electrolytes for CZE analysis of anions. Peaks 1 and 2 symbolize inorganic anions; peaks 3-5 represent short-chain carboxylates; and peaks 6 and 7 represent short-chain alkanesulfonates. Chromate (high mobility), phthalate (intermediate mobility), and p-hydroxybenzoate (low mobility) are examples of the IPD co-ions. The arrow indicates mobility of each IPD reagent [50].

Table 1.1 Advantages and Disadvantages of GC, HPLC, and CE Instruments for SMCFA Analysis

Instrument	Advantages	Disadvantages
GC	• Highly volatile SCFA to be readily separated by GC • Derivatization-involved method provides better resolution, higher sensitivity, and thermal stability	• Multistep sample pretreatment required (filtration, distillation, acidification, extraction, etc.) • Labor-intensive • Extensive auxiliary equipment • Potential loss of FA during pretreatment procedure • Derivatization is needed to increase the volatility of MCFA as well as the thermal stability of SMCFA
HPLC	• Not require high temperature to carry out the separation • Compounds with lower volatility (MCFA) or thermally labile able to be determined	• Multistep sample pretreatment required • Derivatization of SMCFA needed for optical detection due to lack of chromophores and for MS detection due to the low mass range of SMCFA • High risk of column contamination
CE	• Simple sample preparation • No derivatization needed • Low consumption of buffer, reagents, and capillary • A small amount of sample needed • Relatively low cost	• Matrix complexity might affect identification and quantification • Lack of repeatability are often encountered

2 SEPARATION OF SHORT AND MEDIUM-CHAIN FATTY ACIDS USING CAPILLARY ELECROPHORESIS WITH INDIRECT PHOTOMETRIC DETECTION: PART I: IDENTIFICATION OF FATTY ACIDS IN RAT FECES

2.1 Introduction

Short and medium-chain fatty acids (SMCFA) are natural compounds present in the plant, animal, and human cells that play crucial roles in metabolism and the immune system. For instance, in plants, SMCFA acts like defensive agents against insect herbivores and pathogens [1]. SMCFA is generally known as metabolites produced by gut microbiota in animals and humans, which function as intestinal health protectors. Many studies have shown a direct link between SMCFA and various diseases such as diabetes, obesity, cardiovascular diseases, hypertension, depression, inflammatory bowel disease, diarrhea, and brain diseases [2, 3]. The chemical structure of SMCFA is composed of the carboxylic acid head group with an aliphatic chain of one to five carbons (short-chain) and six to twelve carbons (medium-chain). They are produced by the gut microbiota through fermentation of undigested carbohydrates, except for branched-chain fatty acids (FAs), originating from the breakdown of proteins and amino acids. The SCFA (i.e., C_2 –C_5) are known as energy-supplying fuel for colonocytes [4, 5], an anti-inflammatory agent for the intestinal tract [4, 5], and also able to regulate blood pressure in both rodents and humans [6]. On the other hand, MCFA (C_6-C_{12}) facilitates gastrointestinal hydrolysis and absorption as well as beta-oxidation in the liver, which promotes catabolism and impedes tissue storage [7], leading to more energy dissipation and less risk of developing diabetes.

The analysis of SMCFA is essential because these FFAs signal from the gut to communicate with the brain. As mentioned above, they are produced through bacterial fermentation and may play a role in managing inflammatory bowel disease and irritable bowel syndrome. Due to a significant impact on human health and disease treatment, there has been an increasing interest in developing and improving methods to identify and quantify SMCFAs in the gut through various models like rodents, pigs, canines, and humans. There is a need to develop an excellent qualitative or quantitative low-cost measurement of SMCFAs in clinical laboratories daily. As reviewed recently by Primec et al. 2017 [3] and Fiori et al. 2020 [8], the most commonly used method to date is gas chromatography coupled with flame ionization detector (GC-FID) or hyphenated with mass spectrometry (GC-MS). However, both GC-FID and GC-MS have several disadvantages. The GC system has a high risk of being overloaded by impurities, especially non-volatile particles such as biological samples that usually have complex matrixes at various compositions, contaminating the GC column and reducing column life span. On the other hand, time-consuming derivatization needs to form an ester of SMCFA to yield sufficiently intense ions in GC-MS. Moreover, the derivatization might cause an incomplete reaction, by-products, or loss of the target compounds. Some other alternative methods, such as high-performance liquid chromatography (HPLC) and nuclear magnetic resonance (NMR), have been employed for the analytical detection of SMCFA [3, 8]. Like GC, HPLC-UV or HPLC-MS is also engaged in sample pretreatment to prevent column contamination and the derivatization of non-chromophoric SMCFA to improve signal sensitivity. The NMR application on feces

samples has been reported concerning microbiota, but the instrumentation cost and instrument sensitivity are the main choking points of this technique.

Although SCFA has been reported using capillary electrophoresis (CE) with indirect photometric detection (IPD), to the best of our knowledge, there are no reports on the combined separation and detection of SMCFA in a single run. For example, various IPD reagents such as benzoic acid [9, 10], 2,6-pyridinedicarboxylic acid [11, 12], trimellitic acid [13-15], 2,6-naphthalenedicarboxylic acid [16], naphthalene di and tri-sulfonate as well as chromate [17] have been used in the analysis of SCFA but not for the medium-chain fatty acids. This CE method with IPD of SMCFA has the advantage of simple fecal preparation and no derivatization. Besides, the requirement for a small amount of fecal sample and low consumption of buffer and reagents make this potentially a low-cost method. Additionally, the IPD protocol is repeatable to allow its real-world use in clinical settings. Given that MCFAs are reported to be present in fecal samples [5, 18], in this work, we propose a new IPD reagent, 5'-adenosine monophosphate (5'-AMP), for the simultaneous separation and detection of both straight and branched SMCFAs. The 5'-AMP is reported for various non-UV absorbing ions [19-21] but not for the separation and detection of SMCFAs. Various operating buffer compositions, such as the IPD reagent, complexing agent, organic solvent, and non-absorbing BGE concentration, as well as the applied voltage, were varied to obtain an optimal separation. Finally, the method was applied for analyzing SMCFA in adult versus adolescent rat fecal supernatant.

2.2 Experimental

2.2.1 Chemicals and Reagents

Acetic acid (AA, ACS reagent, ≥99.7%), propionic acid (P.A., ACS reagent, ≥99.5%), butyric acid (BA, ≥99%), isobutyric acid (IBA), trifluoroacetic acid (TFA), boric acid (H_3BO_3, SigmaUltra, minimum 99.5%), adenosine 5'-monophosphate sodium salt (5'-AMP, from yeast, ≥99%), and sodium hydroxide solution (NaOH, 50% in H_2O) were purchased from Sigma-Aldrich (St. Louis, MO). Valeric acid (VA, 99%), isovaleric acid (IVA, 98%), and methanol (MeOH, ultrapure, HPLC Grade, 99.8+%) were purchased from Alfa Aesar (Haverhill, MA). Hexanoic acid (HxA, 99%), heptanoic acid (HpA, 98%), and octanoic acid (OA, 99%) were obtained from Acros Organics (Fair Lawn, NJ). Alpha cyclodextrin (α-CD) was purchased from Cerestar USA., Inc. (Hammond, IN). Triply deionized (TDI) water was obtained from the Barnstead Nanopure II water system (Barnstead International, Dubuque, IA, USA).

2.2.2 Buffer Preparation

A start-up condition for the running buffer used in this experiment contained 100 mM boric acid adjusted to pH 6.50. This buffer concentration and pH were used to optimize the concentration of 5'-AMP, α-CD, and MeOH. To prepare 250 mL of 100 mM boric acid (m.w. 61.83 g/mol), an amount of 1.5457 g boric acid was weighed and transferred to a 250-mL beaker. A volume of 220 mL TDI water was added into the beaker, which was sealed with parafilm, placed into an ultrasonic bath, and sonicated for one hr to have boric acid completely dissolved. Next, the pH of this solution was adjusted to 6.50 (± 0.01), first using concentrated (1 M) NaOH and then using diluted (0.1 M) NaOH dropwise. The pH meter was calibrated using standard buffers at pH 4.0,

7.0, and 10.0. The adjusted pH solution was transferred to a 250-mL volumetric flask, added up to the mark with TDI water, sonicated, and degassed for 15 min and 5 min, respectively.

To prepare the running buffer, a certain amount of 5'-AMP (m.w. 347.22 g/mol) was dissolved in 20 mL of 100 mM boric acid buffer in a 30-mL beaker, sealed with parafilm, and sonicated for 5 min. Next, a certain desire amount of α-CD (m.w. 972.84 g/mol) was added into the beaker, sonicated again for at least 30 min for complete dissolution. However, a longer sonication time may be needed if the 5'-AMP and boric acid concentrations increase in the buffer solution. Nonetheless, the pH of the buffer solution was readjusted with 0.1 M NaOH dropwise. The beaker's content was quantitatively transferred to the 25-mL volumetric flask, shake, dilute to the mark, and sonicate again for another 30 min. For buffer containing 7.5% (v/v) MeOH, an aliquot of 1,875 μL of MeOH was transferred into the 25-mL volumetric flask before adding the aqueous content into the flask. The mixing and sonication were done using the same procedure as discussed above. All buffer solutions were filtered with a 0.22-μm nylon syringe filter (Tisch Scientific, OH).

2.2.3 SCFA an MCFA Standard Solutions Preparation

The stock solutions of SCFA, such as AA, PA, BA, IBA, VA, IVA, and MCFA, such as HxA, HpA, OA, as well as the internal standard, TFA, were prepared at 10 mM in TDI water. Separate aliquots of neat 2.86 μL AA, 3.75 μL PA, 4.62 μL BA, 4.62 μL IBA, 5.44 μL VA, 5.45 μL IVA, 6.31 μL HxA, 7.15 μL HpA, 7.92 μL OA, and 3.85 μL TFA were pipetted into their respective stock vials, which were all diluted with TDI water (except for HpA and OA which require 5 μL of 18.9 M NaOH for dissolution) to the final

volume of 5 mL followed by vortex for 1 min. Next, a mixture of all ten acids was prepared by taking an aliquot of 50 µL of each of the stock acids and vortex for 1 min. The standard mixture was filtered with a 0.22-µm syringe filter before transferring 100 µL to the CE vial.

2.2.4 Fecal Sample Preparation

The frozen rat feces were thawed to room temperature for 15 min. Next, feces were weighed out before being placed into the desiccator to remove extra moisture. After 30 min, they were taken out of the desiccator and weighed again. A volume of 1000 µL TDI water was added to each sample, vortexed for 3 min, and centrifuged for 20 min at 14.8 x1000 rpm and 4˚C (model Sorvall^{TM} Legend^{TM} Micro 21R, Thermo Scientific, MA, USA). The supernatant was transferred to a Spin-X® centrifuge filter tube (0.22 µm Nylon, Costar, Corning, NY) and centrifuged at the same condition to remove extra particulates. Eventually, the supernatant was mixed with IS (TFA, 2 mM) before analysis.

2.2.5 CE-UV Instrumentation

The CE separation was performed on Agilent 7100 capillary electrophoresis instrument equipped with a UV detector at a 30 kV power supply. The capillary column used was bare fused silica with an average internal diameter of 75 µm (356 µm OOD), obtained from Polymicro Technologies (Phoenix, AZ). The capillary ends were polished using a polyimide cutter to get smooth flat ends with a total length of 64.5 cm. The column was burnt at 8.5 cm from the capillary outlet to create a UV detection window and inserted into the CE cartridge. First, the capillary was inserted into an alignment

interface in such a way that the detection window was under the lens. Next, it was rolled around the holder until both ends of the capillary were aligned together.

All new capillary columns were rinsed with 1 M NaOH for 30 min, followed by TDI water for 15 min, using high-pressure flush at 2 bar. Pre-conditioning was set as a 5-min flush with prepared buffer solution. Post-conditioning was set as 2-min flush with TDI water, 2-min 1 M NaOH, and 2-min TDI water, all using high pressure at 2 bar. To convert the negative peaks of IPD as positive peaks, the signal wavelength was set at 320 nm, bandwidth at 10 nm, reference wavelengths at 229 nm, 230 nm, 240 nm, 254 nm, 259 nm, 260 nm, and 274 nm, and reference bandwidth at 60 nm. Agilent MassHunter Workstation Data Acquisition and Agilent MassHunter Qualitative Analysis B.07.00 were used for data analysis and instrument control.

2.3   Results and Discussion

2.3.1 Optimization and Separation Parameters for SMCFA

Short (C_2-C_5) and medium (C_6-C_{12}) chain fatty acids (SMCFA) are composed of an aliphatic tail and a monocarboxylic group with pKa values ranging from 4.75-4.89 (Fig. S1), making them ionizable in aqueous solution. However, MCFA needs a strong base or organic solvent to solubilize. In this study, the separation of four straight-chain (C_2 –C_5), three of the medium-chain (C_6-C_8), and two branched-chain (IBA and IVA) FAs were optimized using 5'-AMP as IPD reagent. The TFA is an organofluorine compound, a structural analog of SCFA, and was selected as an internal standard (IS) in the test mixture. Five main studies were conducted to optimize the separation of nine SMCFAs. First, an organic solvent, methanol, was added to the running buffer to resolve the FAs from the system peak and to improve the overall separation. Second, a complexing

agent, *α*-CD, was utilized to determine the two isomeric pairs, BA/ IBA and VA/IVA, in the SMCFA mixture. Third, the type of chromophore and concentration of optimized chromophore (i.e., 5'-AMP) was investigated to obtain the best *S/N* ratio of the FAs. Further study on varying concentrations of boric acid as a BGE was also implemented. Finally, the applied voltage was examined to determine the effect of joule heating on the separation of SMCFA.

2.3.1.1 Effect of Methanol

The use of 5'-AMP has been investigated previously to separate low mobility anions in various publications [22-24]. Initially, 5'-AMP was investigated as a reagent for IPD involving separation of nine SMCFAs with the addition of boric acid and α-CD but without MeOH (Fig.2.1A). As mentioned earlier, SMCFA having a range of p*Ka* around 4.75-4.89 are all negatively charged in the running buffer at pH 6.5. Capillary ion electrophoresis (CIE) separates non-UV absorbing molecules not only by charge-to-size ratio, but the peak shapes are also essential. Therefore, their elution order is determined by their size difference. The longer the anionic chain of the FAs, the slower its mobility towards the anode and vice versa. As a result, the electroosmotic flow (EOF) drives the longer chain FAs towards the detector's cathodic end faster than the shorter ones. Because the structures of the isomeric pairs (straight vs. branched) of C_4 and C_5-FAs have the same electrophoretic mobility, the presence of *α*-CD in the BGE enhanced the resolution between the pairs. The increasing elution order of all SMCFAs migration time are observed as follows: OA < HpA < HxA < VA < IVA < BA < IBA < PA < AA, which was verified by the automated spiking method (Appendix A, Fig.S2.2).

In CIE, the shape of an analyte zone that migrates in a BGE (containing IPD reagent) depends on the electrodispersion, which results in symmetric or asymmetric peak shape, fronting, or tailing pattern. Fronting peaks are caused when the mobility of FA is higher than the mobility of the IPD reagent, while the converse mobility mismatch results in tailing peaks. As seen in Fig. 1A, AA and PA peaks are tailing ($As > 1.0$) under positive polarity, indicating their mobilities are higher than 5'-AMP. On the contrary, all other SMCFA peaks are fronting ($As < 1.0$), meaning their mobilities are lower than 5'-AMP. Because the wide range of FAs with different mobility from C_2 to C_8 were simultaneously resolved, the slight mismatch between 5'-AMP mobility and SMCFA mobilities is negligible. Although all the SMCFA and TFA were baseline separated, the VA (peak 4) coeluted with the negative system peak (SP).

The use of organic solvent has many benefits in CIE, including the ability to alter buffer viscosity as well as conductivity to resolve the coelution of peaks. The electropherogram in Fig.2.1B demonstrates a substantial improvement in resolution of VA and SP when 7.5% (v/v) of MeOH was added into the running buffer at the expense of a 5 min increase in total run time. Even though the analysis time was longer with the use of MeOH, overall, the resolutions of all SMCFA were improved. The presence of MeOH reduced the buffer's conductivity due to a decrease in EOF, leading to a good separation of VA and SP. The use of 7.5% (v/v) of MeOH was optimum because a lower percentage of MeOH provides lower resolution of VA and SP, whereas a higher percentage of MeOH results in a very long run time (data not shown).

2.3.1.2 Origin of System Peak

The mechanism of the generation of SPs in both ion chromatography (IC) and CIE is rather complex [25]. Several researchers have established the basic principles of SP origin in ion chromatography [26]. We hypothesize that the origin of the system peak is due to the presence of UV-absorbing impurity in the IPD reagent (5'-AMP). To test this hypothesis, 5'-AMP was prepared at two different concentrations using the same BGE recipe optimized in Figure 2.1B. In the first experiment, using 3 mM of 5'-AMP, spiking the standard mixture with 50 mM boric acid did not increase the size of the system peak (Appendix A, Fig.S2.3A vs. B). Next, the spike was performing using 1 mM of 5'-AMP, and 50 mM boric acid, only a slight increase in the size of SP was observed, but the direction of SP remained unchanged (Appendix A, Fig.S2.3C). Obviously, in the absence of 5'-AMP in the running buffer, no peaks are detected upon injecting a standard SMCFA mixture, but the SP is also not detected (Appendix A, Fig.S2.3D). In the second experiment using 5 mM of 5'-AMP in the BGE, first, the standard mixture (Appendix A, Fig.S2.4A) was injected, and the same mixture was spiked with water in the next injection (Appendix A, Fig.S2.4B). The SP size remains unchanged when spiked with water. In the third and fourth injections, the standard FA mixture was spiked with low and high concentrations of 5'-AMP (Appendix A, Fig.S2.4C and D). Still, an increase in peak area and the peak height of SP proportional to the increase in injection concentration of 5'-AMP was observed. Thus, it is reasonable to believe that one reason for the origin of SP in IPD is the light-absorbing impurities present in the reagent (i.e., 5'-AMP).

2.3.1.3 Effect of Alpha-cyclodextrin Concentration

One of the most commonly used complexing agents added to the CE buffer is CD. The three most common types of CD are α-CD, beta(β)-CD, and gamma (γ)-CD, which is comprised of six, seven, and eight glucopyranose units, respectively, linked through the α-1,4-glucosidic bond. Because of a different number of sugar units, the hydrophobic central cavity has different diameters, and a hydrophilic outer surface increases the number of primary hydroxyl groups. The recognition ability of various CDs depends on how well the hydrophobic molecules fit inside the cavity. The inclusion complexation of analytes with CD usually occurs in aqueous media. Small functional groups like linear alkyl group of FAs are favorably complexed better with α-CD in comparison to β-CD and γ-CD due to the smallest cavity size of α-CD [27]. Additionally, it is well-known that α-CD prefers complexing with simple anionic species than cationic [27]. With those characteristics, α-CD was chosen to add into the running buffer to separate two isomeric pairs (i.e., BA/ IBA and VA/ IVA) in the SMCFA mixture.

Several trends are noted when comparing the separation of nine SMCFA and the IS (Fig.2.2 A – E) upon increasing the concentration of α-CD. First, the migration time of the SMCFA reduced in the presence of α-CD and continued to shorten upon increasing α-CD concentration. As a neutral complexing agent, α-CD moves along with the EOF toward the cathode. When being complexed with neutral α-CD, anionic FAs will slow down because of the heavier mass. Accordingly, the EOF dragged the FA-α-CD anionic complexes faster than the uncomplexed form to the detector end. Besides, when comparing the migration time of SMCFA upon the addition of 3 mM α-CD, MCFA eluted relatively more quickly than SCFA. A recent review of CD's inclusion behavior

suggested that CDs have a hydrophobic cavity [27]. Our result indicated that the longer the chain of the FAs, the higher the hydrophobicity, consequently greater the complexation with the α-CD. Therefore, the migration times of MCFA were drastically declined when α-CD was added into the running buffer (Fig.2.2 A and B). For example, HpA was eluted at 8.3 min and 6.4 min, respectively, without and with 3 mM α-CD. On the other hand, AA's elution was not significantly different as this compound eluted at 14.2 min and 13.6 min, respectively. Further addition of α-CD to 7 mM reveals that the repeatability of migration time was very poor. For example, as shown in Table S2.1 (Appendix A), the %RSD of migration time was less than 4% in the 3-5 mM concentration range. However, at 7 mM, %RSD was not only higher (6-16%), but for SCFA, the repeatability was even worse compared to MCFA.

Second, the improvement of resolution between straight and branched-chain FAs was quite evident. The elution order was determined by automated spiking injections, which showed that the straight chain of both C_4 and C_5 FAs eluted faster than their branched versions (Appendix A, Fig.S2.2). For example, BA eluted before IBA, and VA eluted before IVA. This result agreed with the previously reported data that α-CD cavity preferably includes linear alkyl chain [27]. Third, the SP overlapped with either OA, HxA, or VA without (Fig.2.2A) and with the presence of variable α-CD concentration (Fig.2.2 B and C). The overlapping issue was completely resolved as α-CD concentration was raised up to 5 mM (Fig.2.2D). Further increasing concentration of α-CD to 7 mM (Fig.2.2E) provided greater resolution between HxA and SP, VA moved closer to the SP (Fig.2.2. inset plot). Therefore, 5 mM seems to be the best concentration of α-CD for separating all SMCFA without any overlap with the SP.

2.3.1.4 Effect of Chromophore Type and Concentration

Initially, four IPD reagents, including para-hydroxybenzoic acid (PHBA), 5'-AMP, naphthalenemonosulfonic acid (NMS), and 3-nitrobenzoic acid (NBA), were tested for the separation of SCFA. All four chromophores provided baseline separation, but 5'-AMP provided the most stable baseline with a well-resolved SP from the FA peaks (Appendix A, Fig.S2.5). Although NBA, NMS, and PHBA provided baseline separation for each SCFA, very unstable baselines were seen in all three electropherograms (Appendix A, Fig.S2.5 A, C-D), perhaps due to low molar absorption coefficients (5,960 L/mol·cm [28], 6,200 L/mol·cm [29], and 14,000 L/mol·cm [30] for three probes, respectively) compared to 5'-AMP (15,400 L/mol·cm [31]). Additionally, imperfect peak shapes with numerous satellite SP suggest significant chromophoric reagent impurities. Because 5'-AMP provided higher efficiency and resolution for separating model FAs, it was determined to be the best IPD reagent for separating and detecting SMCFA.

In addition to the molar absorptivity and electrophoretic mobility, the IPD reagent concentration is also a key factor because it can affect the dynamic reserve (DR) that influences peak efficiency and resolution. Lowering the concentration of the IPD reagent will attain a lower concentration limit of detection. Still, there is also a risk of lessening dynamic reserve, which can cause an increase in background noise and poor peak shape, affecting peak efficiency and resolution. Varied concentrations of 5'-AMP from 3 to 9 mM were examined. As shown in Fig.2.3A, there is a general trend of a slight increase in relative migration time (t_r/t_0) and t_0 values for all SMCFA except AA. Additionally, a higher concentration of 5'-AMP favored the greater resolution of critical pairs, including HpA/HxA, VA/IVA, and BA/IBA (Fig.2.3B). Still, AA's longer migration

time is the determining factor in finding an appropriate 5'-AMP concentration (Appendix A, Fig.S2.6). A further experiment was conducted using a much narrower range of 5'-AMP concentration (i.e., 7, 8, and 9 mM) to determine if 8 mM 5'-AMP could better resolve FAs than 7 mM (Fig.2.3B) but with a considerably shorter analysis time than 9 mM. The result agreed with our prediction (Appendix A, Table S2.2a). Moreover, there was a decrease in the efficiency of SMCFA at the concentration of 9 mM 5'-AMP (Fig.2.3C). This efficiency trend is consistent with the *S/N* ratio data shown in Table S2b (Appendix A), where the *S/N* ratio for the SMCFA was more significant at 8 mM than 9 mM. Increasing 5'-AMP concentration experienced a decrease in the *S/N* ratio because of the direct proportionality between IPD reagent concentration and the concentration limit of detection. The resolution of SMCFA was highest at 9 mM due to a more significant impact from an increase in selectivity (α) in SMCFA (Appendix A, Table S2a). Similar to chromatography, substantial improvement of resolution is expected in CE even when there is a slight change in *α*-value. Eventually, 8 mM 5'-AMP was a good compromise in terms of migration time, resolution, and efficiency for the separation of SMCFA.

2.3.1.5 Effect of Boric Acid Concentration

The running BGE utilized in this experiment is boric acid (H_3BO_3). It is well-known that the BGE concentration directly influences the CE separation by altering the ionic strength and EOF. Therefore, a range of H_3BO_3 from 50 to 150 mM was examined to seek the best H_3BO_3 concentration that improves peak shape while still maintaining a rapid analysis time for SMCFA. Initially, the migration time of the SMCFA remained unchanged upon an increase in H_3BO_3 concentration from 50 to 100 mM (Fig.2.4A-C).

At the concentration of 125 mM, there was a substantial increase in total analysis time from 15 to 20 min (Fig.2.4D). The increase in ionic strength can reduce the electrical double layer's thickness in the capillary, causing a drop in zeta potential. The magnitude of EOF is directly proportional to zeta potential. Thereby, the EOF slowed down, increasing the migration time of the analytes in the capillary. However, at 150 mM H_3BO_3, the migration time of all FAs dropped (Fig.2.4E). We hypothesized that this decrease in migration time is related to joule heating. To test our hypothesis, experiments were performed to study the current-voltage relationship at both 100 and 125 mM H_3BO_3. Clearly, the inset plots demonstrated a decrease in the R^2 value from 0.9996 to 0.9988 (Fig.2.4 inset plot a), indicating some joule heating happened inside the capillary. Besides, it is observed that the resolution of SP and the two FAs (HxA and VA), eluting close to the SP, reaches the greatest value at 100 mM compared to 50 and 75 mM H_3BO_3 (Fig.2.4 inset plot b). Therefore, 100 mM H_3BO_3 was selected as the optimum concentration for the separation of SMCFA.

2.3.1.6 Effect of Applied Voltage

Another operating parameter that significantly affects CE separation is applied voltage, which determines the magnitude of the running buffer electric field strength, which is directly proportional to EOF, during the separation. Typically, the effect of voltage is the last parameter that is optimized in CE separation. It is evident in Fig. S2.7 (Appendix A) that increasing voltage from 10 kV to 30 kV shortened the run time from 36 min to 13 mi (almost threefold). Additionally, higher voltages sharpened the peak shape of the analytes. The inset plot in Fig.S2.7a (Appendix A) showed that a t_r/t_0 was not affected by a voltage change. In contrast, there was a rapid decline in dead time (t_0)

as the voltage increased (Appendix A, Fig.S2.7 inset plot b), which implies increasing voltage speeds up the EOF solely without altering the analytes' electrophoretic mobilities. This trend is consistent with the fundamental equation, which directly relates EOF to applied voltage [32]. Overall, the apparent mobilities of the analytes increased, causing them to elute faster at higher voltages. There was no significant difference in the efficiency of the FAs at varied voltages, except for the efficiency of the IBA peak, which was significantly enhanced at higher voltages (Fig.2.5). Perhaps, IBA has mobility very similar to electrophoretic mobility of 5'-AMP. Thus, the maximum voltage of 30 kV was used in consideration of the shortest analysis time and satisfactory efficiency.

2.3.2 Application of SMCFA in Biological Samples

The developed CE-IPD method was applied to qualitatively screen SMCFA in rat feces. As shown in Fig.S2.8 (Appendix A), comparing unspiked and spiked electropherograms of fecal solution (FS) reveals an increase in peak area and the peak height of seven out of nine SMCFAs in rat FS. Although several peaks (marked with an asterisk) were not identified, they were all well resolved from SMCFA. Furthermore, the most abundant FA was AA, followed by PA and BA. Other FAs, including IBA, VA, IVA, and HxA, were also present but only at very low concentrations. A comparison of adult versus adolescent rat's fecal supernatant was also profiled (Fig.2.6). Interestingly, only AA was detected in adolescent rat FS (Fig.2.6A), whereas the adult rat (Fig.2.6B) contained all SMCFA. Due to the absence of most SMCFA in adolescent rat FS, except for AA, the adolescent rat FS could be used as a blank for quantitation. For example, standard FAs could be spiked at different concentrations in adolescent fecal solution

allowing to generate a calibration curve for better matrix matching. Therefore, the concentration of unknown samples can be obtained with higher precision and accuracy.

To ensure the accuracy of the proposed CE-IPD method, recovery experiments were performed by adding a certain amount of SMCFA mixture standards to the rat fecal solution. The recoveries at three levels of concentration are summarized in Table 2.1. An excellent intra-day and inter-day precision for relative migration time (t_r/t_0) and peak areas were achieved at all three concentration levels. The RSD values of t_r/t_0 did not exceed 2%, except for AA (4%) at a low concentration level in an inter-day measurement. For peak area, the %RSD at three concentration levels were all below 15%. As a result, the proposed CE-IPD method demonstrated adequate SMCFA separation and detection in FS. Reported demonstrated

2.4   Concluding Remarks and Future Directions

A simple, cost-effective, and straightforward CE-IPD method is developed for SMCFA that could be applied to quantitate SMCFA in rat feces. A new buffer recipe composed of 5'-AMP combined with α-CD and MeOH in the BGE was tested to optimize the simultaneous separation of straight and branched fatty acids. The complexing agent, α-CD, was a critical factor in achieving the resolution of two isomeric pairs, BA/IBA and VA/IVA. The IPD reagent, 5'-AMP, demonstrated a stable baseline and highest efficiency for SMCFA than the other three IPD reagents (PHBA, NMS, and NBA). The studies on the concentration of 5'-AMP and H_3BO_3 and MeOH revealed their essential roles in enhancing the resolution between SP and the two nearby FAs, HxA and VA. A baseline separation of all nine SMCFA was achieved under IPD buffer

conditions such as 5 mM α-CD, 8 mM 5'-AMP, 7.5% (v/v) MeOH, 100 mM H_3BO_3, and 30 kV in 15 min.

Our results showed good repeatability when separating standard FAs in a biological matrix such as rat fecal supernatant. The intra-day and inter-day precision assay illustrated %RSD below 2% for migration time and below 15% for peak area. The preliminary study on SMCFA in rat feces reveals an interesting finding where SMCFA from C_2 to C_6 were detected in adult rats, but only C_2 (AA) in adolescents. This noteworthy observation suggests that further method validation and quantitation are warranted for a larger pool of samples to elucidate the association between the production of SMCFA in rats of different ages and their gut health conditions.

This developed assay has strong potential to exert a significant impact in basic and clinical research, as well as diagnostics and treatments. The assay will be fully validated in Part II for measuring (SMCFAs) in rat feces to meet the need of neuroscientists and clinical researchers interested in the role of SCFAs in organismal function. We will expand the scope of this low-cost CE-IPD platform, which requires minimal pretreatment procedures and nanomole quantity of biospecimen. Specifically, we will develop the assay in the context of investigating the role of the gut-brain axis in addiction. We will use rats (*Rattus norvegicus*) as the animal model and cocaine as the addictive compound. Preliminary results suggest that oral antibiotics deplete bacterial populations in the gut of adolescent and adult male rats, and this depletion is associated with heightened reinstatement of cocaine-seeking after abstinence (i.e., relapse), but only in adult subjects [33]. Given that gut bacteria are major producers of SCFAs and exogenous administration of SCFAs to antibiotic-treated adult mice restores normal

cocaine-related behavior [34], we predict that SCFAs quantitated through CE–IPD will be reduced in all rats treated with antibiotics, with more significant reductions in adults than adolescents. The following paper will discuss our findings on these exciting trends.

Table 2.1 Intra- and inter-day precisions of CE-IPD method for SMCFA analysis

FA	Intra-day (RSD)/ % (n=5 each level)						Inter-day (RSD)/ % (3 days, n=15 each level)					
	Low[a]		Medium[b]		High[c]		Low[a]		Medium[b]		High[c]	
	t_r/t_0	Peak area	t_r/t_0	Peak area	t_r/t_0	Peak area	t_r/t_0	Peak area	t_r/t_0	Peak area	t_r/t_0	Peak area
AA[‡]	0.9	10	1	3	2	7	4	8	2	7	2	14
PA	0.9	9	0.9	2	1	-[*]	1	6	1	4	1	-[*]
IBA	0.5	13	0.7	1	1	9	0.6	7	0.9	5	2	13
BA	0.5	12	0.7	2	1	10	0.6	9	0.8	5	2	13
IVA	0.9	12	0.6	0.8	1	10	0.7	6	0.5	10	1	12
VA	1	14	0.6	7	1	7	1	15	0.4	1	1	14
HxA	0.3	10	0.5	2	1	9	0.3	7	0.2	5	2	12

[a]low-level concentration corresponds to 0.1 mM, [b]medium-level 0.5 mM, [c]high-level 1 mM
[*]PA is partially resolved from matrix peak at high-level concentration
[‡]Peak area represents spiked concentration and endogenous concentration of AA in the fecal sample
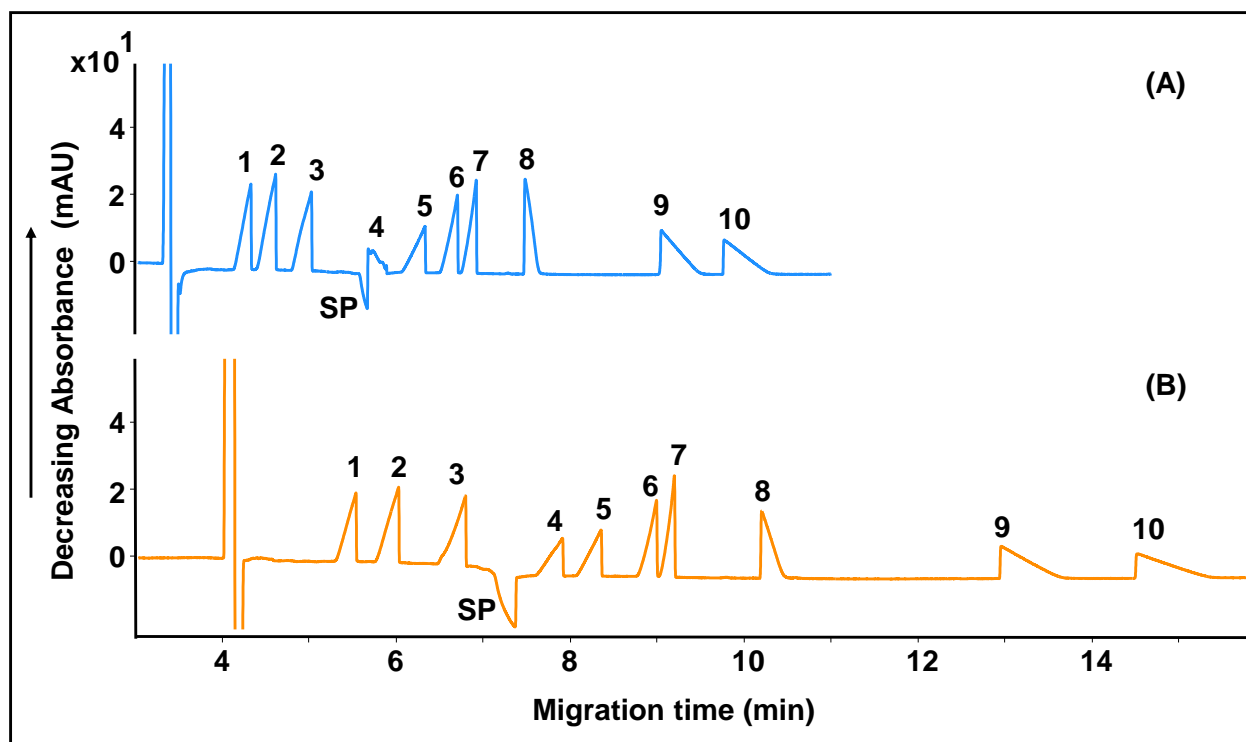
Figure 2.1 Separation of short and medium-chain fatty acids (SMCFA) without (A) and with (B) 7.5% (v/v) methanol using capillary electrophoresis (CE) with indirect photometric detection (IPD). Conditions: Bare fused silica capillary, 75 µm i.d., 56 cm effective length; 100 mM borate buffer containing 7 mM adenosine-5'-monophosphate (5'-AMP), 5 mM alpha-cyclodextrin (α-CD), pH 6.50, 7.5% (v/v) MeOH; injection size 5 mbar 50 s; applied voltage 30 kV (15 µA); UV detection: signal λ at 320 nm, reference λ at 260 nm, bandwidth (10 nm). The arrow indicates the direction of decreasing absorbance. Peak identification: 1 mM each of 1. octanoic acid (OA), 2. heptanoic acid (HpA), 3. hexanoic acid (HxA), 4. valeric acid (VA), 5. isovaleric acid (IVA), 6. butyric acid (BA), 7. isobutyric acid (IBA), 8. propionic acid (PA), 9. acetic acid (AA) , 10. trifluoroacetic acid (internal standard, IS) and SP, system peak.
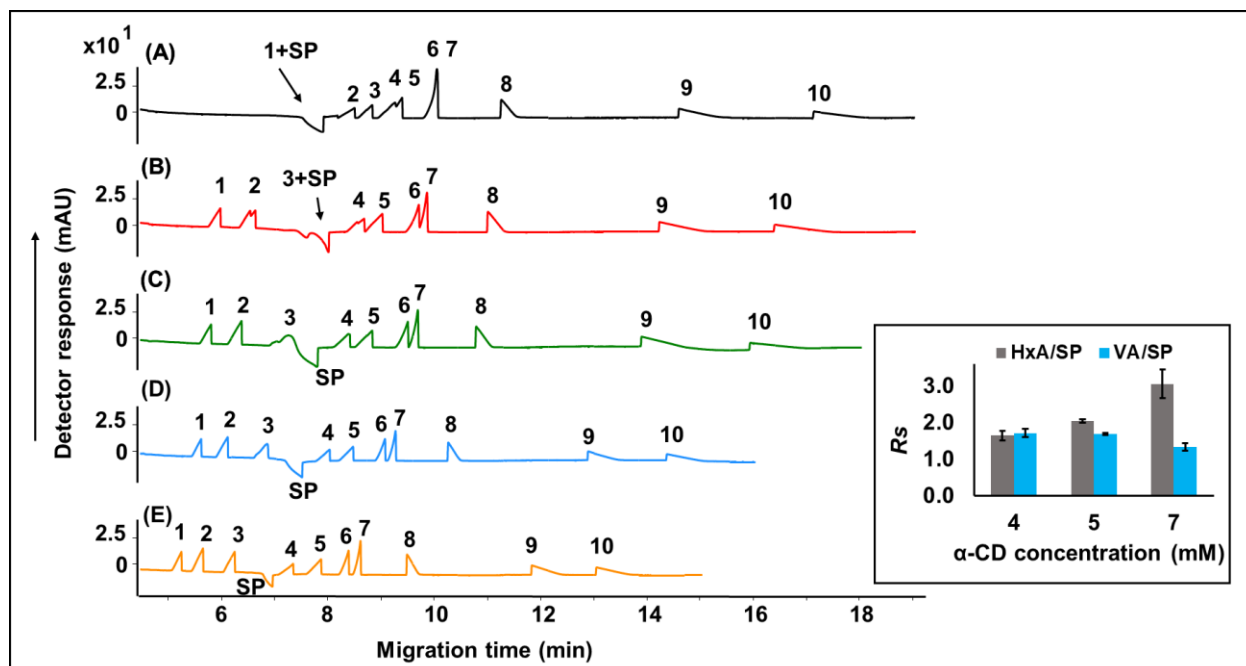
Figure 2.2 Effect of α-CD concentration on the separation of SMCFA using CE-IPD. The CE separation conditions are identical to Fig. 1 except for varied concentration of α-CD: (A) 0mM, (B) 3 mM, (C) 4 mM, (D) 5 mM, (E) 7 mM. Peak identification is the same as Fig.2.1. Inset plot is the resolutions between system peak (SP) and hexanoic acid (HxA) and SP and valeric acid (VA) in an increase of α-CD concentration from 4 mM to 7 mM
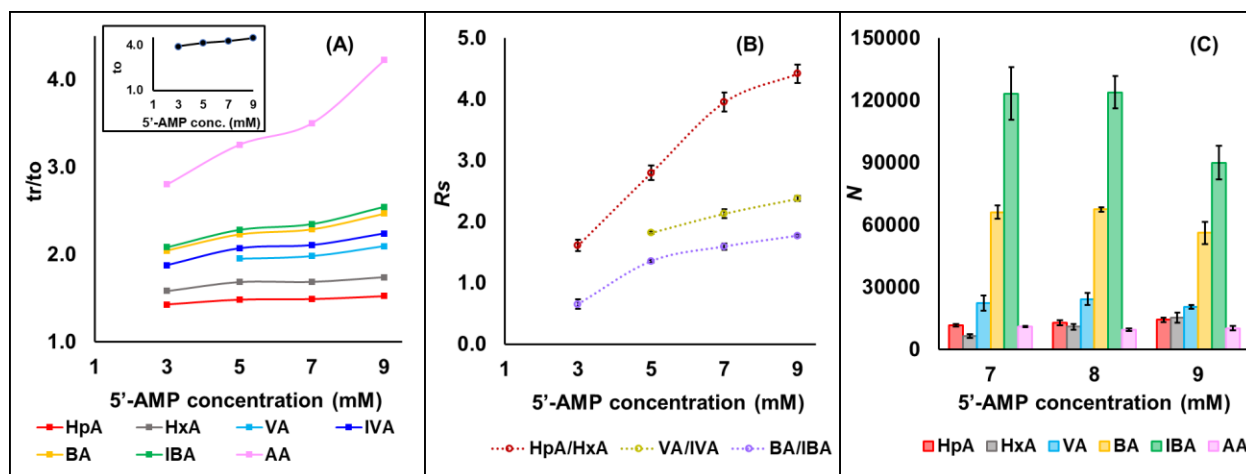
Figure 2.3 Effect of 5'-AMP concentration on (A) t_r/t_o and (B) resolution (Rs) and (C) efficiency of representative SMCFA. CE separation conditions are identical to Fig.2.1. The inset plot in (A) is the EOF as a function of 5'-AMP concentration.
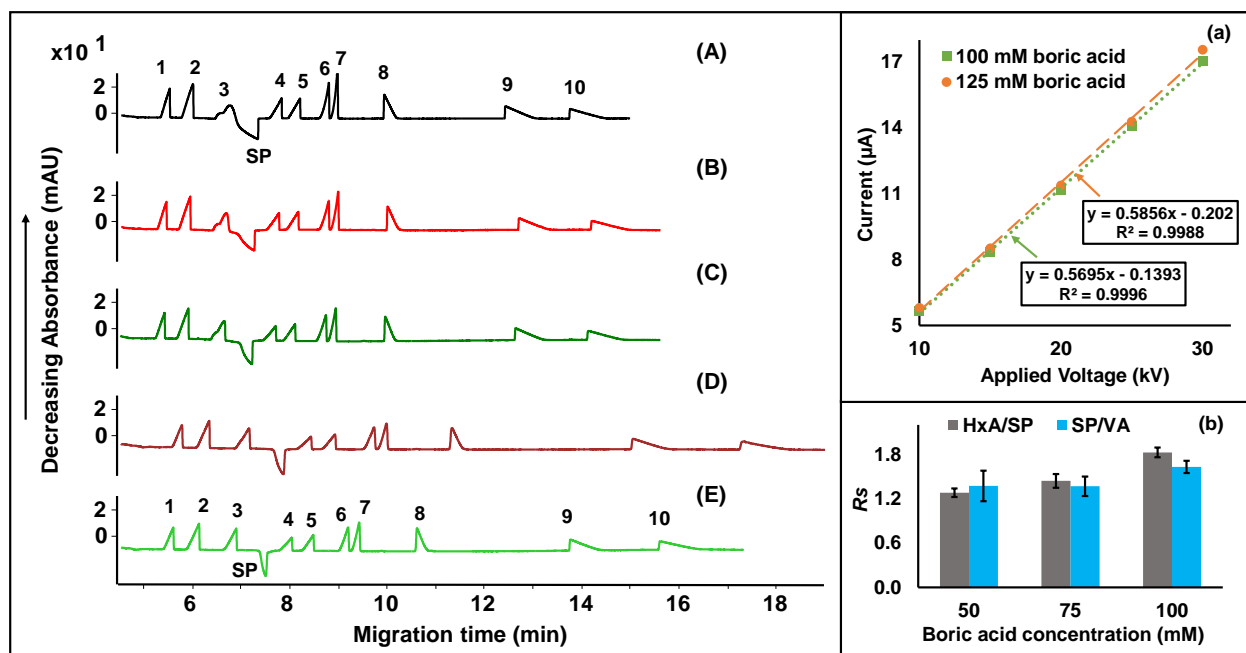
Figure 2.4 Effect of boric acid concentration on the separation of SMCFA using CE-IPD. The CE conditions and peak identification are identical to Fig.2.1 except for 8 mM 5'-AMP and varied concentration of boric acid (A) 50 mM, (B) 75 mM, (C) 100 mM, (D) 125 mM, (E) 150 mM 5'- AMP. The inset plot (a) is the current-voltage curve at 100 mM and 150 mM boric acid. The inset plot (b) is the resolutions between SP and HxA and SP and VA upon increasing boric acid from 50 mM to 100 mM.
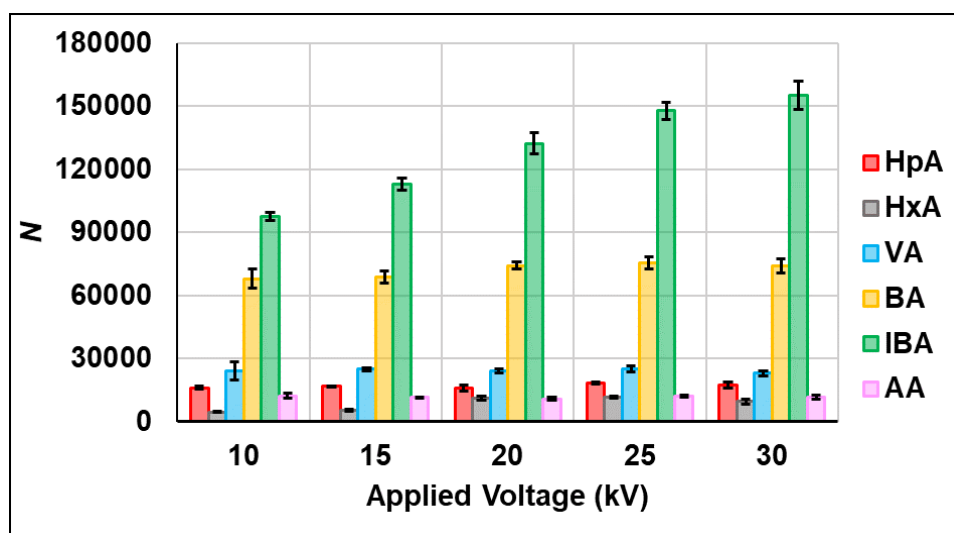
Figure 2.5 Effect of applied voltage on efficiency (N) of six representative SMCFA. CE separation conditions are identical to Fig.S2.6.
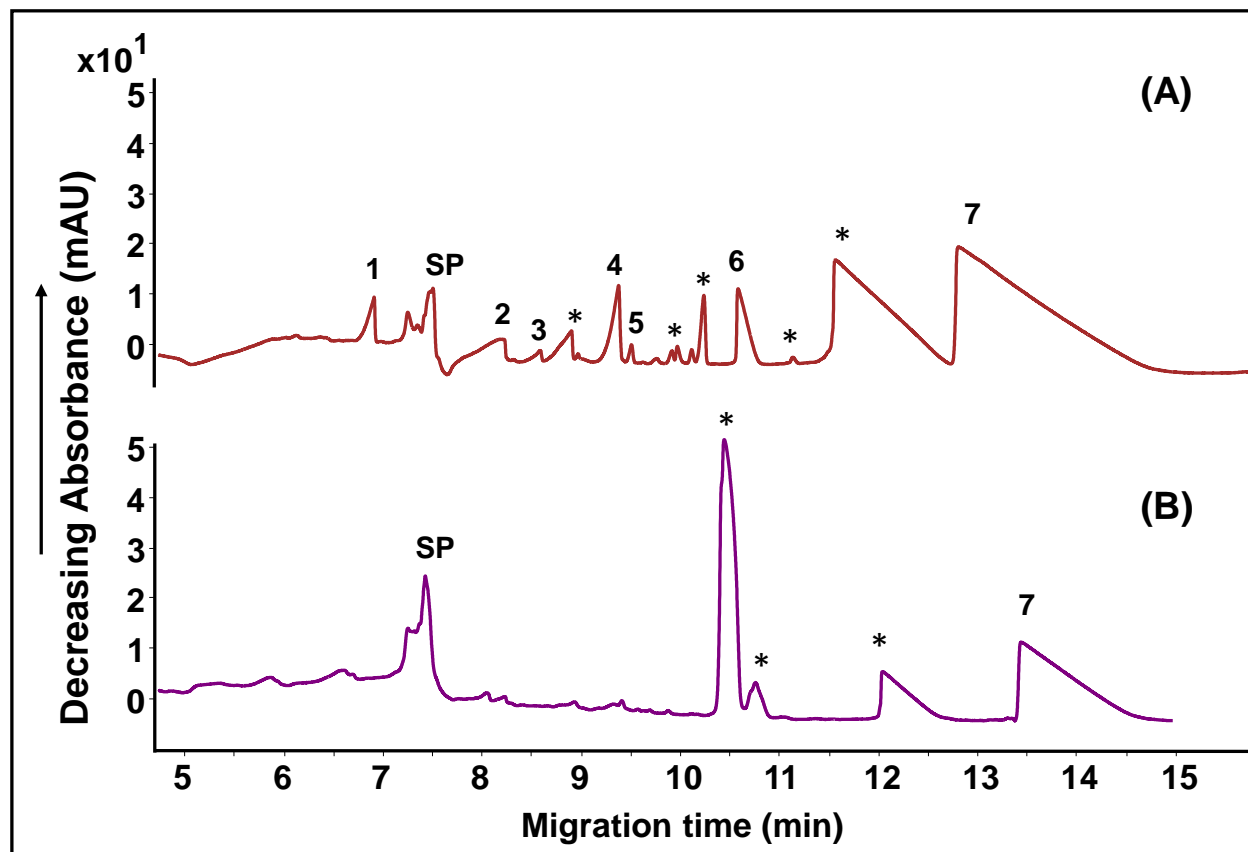
Figure 2.6 A comparison of (A) adult rat fecal solution (FS) and (B) adolescent rat FS. The CE separation conditions are identical to Fig.2.1 except for 7.5% MeOH and 8 mM 5'-AMP. Peak identification: 1. HxA, 2. VA, 3. IVA, 4. BA, 5. IBA, 6. PA, 7. AA. Asterisk-marked peaks are unknown from the matrix. SP is the system peak.

3   SEPARATION OF SHORT AND MEDIUM-CHAIN FATTY ACIDS USING CAPILLARY ELECTROPHORESIS WITH INDIRECT PHOTOMETRIC DETECTION: PART II: VALIDATION AND MEASUREMENT OF ENDOGENOUS CONCENTRATION IN FECES OF CONTROLLED VS. DRUG TREATED RATS

3.1   Introduction

Recently, many studies have gained much interest in the roles of short and medium-chain fatty acids (SMCFAs) on the gut microbiota metabolism, which overall relates to health preservation [1-5]. The SCFAs, including acetic acid (AA), propionic acid (PA), butyric acid (BA), and valeric acid (VA), are reported to be found in rats and human feces. Besides the four main SCFA, the branched-chain [isobutyric acid (IBA), isovaleric acid (IVA)], as well as the medium-chain hexanoic acid (HxA) and heptanoic acid (HpA) are present in lower amounts. These gut microbial end products play a crucial role in preventing and treating several metabolic disorders [6] such as type 2 diabetes and obesity, inflammatory bowel diseases [7], and multiple sclerosis. In addition, in gut-brain communication role of SMCFA is linked to brain disorders such as Alzheimer's and Parkinson's disease [8]. Therefore, it is necessary to understand factors that influence SMCFA production as well as the alteration due to aging, diet, and drug use.

One of the typical drug treatments for bacterial infections is antibiotics. However, there is increasing concern that antibiotic exposure has long-term consequences on the gut microbiota and homeostasis [9-11]. Epidemiological studies revealed that antibiotic-induced disruption of the gut microbiota increased the risk of multiple disorders [12-14], including inflammatory bowel diseases [15, 16]. Recently, Holota and co-authors, who

investigated the antibiotic therapy on the SCFA population and intestinal barrier integrity, found that antibiotic *ceftriaxone* significantly decreased the concentration of SCFA and impaired colonic mucosal barrier and epithelium function, causing the susceptibility to the inflammatory reaction development [10].

Another way to alter the gut microbiota is to study cocaine use disorder and its association to gut health. The depletion of the gut microbiota was found in a recent *in vivo* study, suggesting a possible association between cocaine use and inflammatory gut milieu [17]. Cocaine abuse is also connected with changes in the dopamine neurotransmitter system leading to addiction and other complications like malnourishment and reduced blood flow to the gastrointestinal tract [18].

To date, several gas chromatography (GC) techniques are established for the quantitation of SMCFA in feces, primarily GC with flame ionization detection [19] or GC coupled to mass spectrometry (MS) [20], as well as high-performance liquid chromatography (HPLC) with MS [21, 22]. The GC and HPLC methods provide a high sensitivity of SMCFA. Still, most chromatographic methods require pre-column chemical derivatization and multistep sample pretreatment to improve the volatility, thermal stability, and ionization responses. Alternatively, capillary electrophoresis with indirect photometric detection (CE-IPD) has recently emerged as a microseparation technique without the need for pre-column derivatization. Additionally, CE-IPD provides an alternative to GC and HPLC with low-cost capillaries, minimum sample, and buffer consumption to analyze SMCFA in fecal specimens. To date, few validated CE-IPD methods are reported for quantitation of SCFA in feces. Using benzoic acid as an IPD electrolyte, two reports quantitated SCFA in mice, canine, and human feces [23, 24],

and one paper [25] quantitated three SCFAs in infant feces with inflammatory bowel disease using the combination of three anionic chromophores (naphthalenetrisulfonate, naphthalenedisulfonic acid, and chromate).

There are two primary goals of the studies reported in this chapter. The first goal is to examine the analytical figures of merit for method validation to establish baseline concentration of SMCFA (including branched-chain FAs) in the fecal solution of healthy adult and adolescent rats. Reliable quantitation of feces is challenging because of substantial moisture content. To achieve this goal, a simple, efficient desiccation time is first optimized to obtain dried feces. Next, selectivity, linearity, the limit of detection (LOD), the limit of quantitation (LOQ), recovery, precision, accuracy, matrix effects, and stability are examined. The second goal is to evaluate if CE-IPD is a viable assay to test whether and to what extent the treatment of antibiotics, cocaine, or both depletes the SMCFA content in healthy rats. To the best of our knowledge, this is the first CE-IPD method quantifying fecal SMCFA in healthy adults versus adolescent rats to establish baseline concentrations. Furthermore, the method allows for the differentiation of healthy (control) rats from antibiotic and cocaine-treated rats. For example, assessment of fecal SMCFA levels in both control and cocaine-treated rats may enable a better understanding of the mechanisms of cocaine use disorder and gut dysbiosis because the deteriorating gut health is known to be linked to neurological disorders [17]. Additionally, antibiotics can seriously disturb the balance of SCFA, thereby influencing intestinal function. Thus, SCFA could serve as a marker for a healthy gut [19].

3.2 Experimental

3.2.1 Materials and Fecal Samples

The chemicals and reagents purchased from Sigma-Aldrich (St. Louis, MO) are listed as follows: acetic acid (AA, ACS reagent, ≥99.7%), propionic acid (PA, ACS reagent, ≥99.5%), butyric acid (BA, ≥99%), isobutyric acid (IBA), trifuoroacetic acid (TFA), boric acid (H_3BO_3, SigmaUltra, minimum 99.5%), adenosine 5'-monophosphate sodium salt (5'-AMP, from yeast, ≥99%), and sodium hydroxide solution (NaOH, 50% in H_2O). Valeric acid (VA, 99t%), isovaleric acid (IVA, 98%), and methanol (MeOH, ultrapure, HPLC Grade, 99.8+%) were purchased from Alfa Aesar (Haverhill, MA). Hexanoic acid (HxA, 99%) was obtained from Acros Organics (Fair Lawn, NJ). Alpha cyclodextrin (α-CD) was purchased from Cerestar USA, Inc. (Hammond, IN). Triply deionized (TDI) water was purified from the Barnstead Nanopure II water system (Barnstead International, Dubuque, IA, USA).

Male Wistar rats were housed at 20-25°C with 12/12-hr light/dark cycles (lights off at 7:00 a.m. and lights on at 7:00 p.m.) in the vivarium at Petit Science Center, Georgia State University, with free access to water and food. All of the animal care and procedures were performed according to the protocols and guidelines approved by Institutional Animal Care and Use Committee. Rats were fed with Standard Rodent Feed in a pellet form. The animals were allowed to access antibiotic cocktails (neomycin, bacitracin, and ampicillin) or cocaine over two hours only during behavior testing in the operant chambers. Antibiotic cocktail and cocaine were self-administered via a lever press that was connected to a pump system attached to the animals' jugular

vein catheterization port. The dose was based on the bodyweight taken before behavior testing daily. Rat feces were stored at -80°C until processing.

3.2.2   SMCFA Extraction

The frozen rat feces were thawed to room temperature for 15 min before being weighed and dried in the desiccator. The original fecal pellet was split into six equivalent fractions of approximately 0.119 ±0.002 g into six 1.5-mL centrifuge tubes in the desiccation experiment. Fraction one to fraction six were permitted to sit in the desiccator for 2, 4, 6, 8, 10, and 12 hours, respectively. All samples were placed into the desiccator at the same time. After each appointed time, the corresponding fecal fraction was removed from the desiccator and weighed again to determine the dried content mass. A volume of 700 µL DI water was added to each fraction, vortexed for 3 min, and centrifuged for 20 min at 14.8x1000 rpm and 4°C (model Sorvall™ Legend™ Micro 21R, Thermo Scientific, MA, USA). The supernatant was transferred to a Spin-X® centrifuge filter tube (0.22 µm Nylon, Costar, Corning, NY) and centrifuged at the same condition to remove extra particulates. Finally, the supernatant was stored at -20°C until analysis.

3.2.3   Standard SMCFA and Fecal Sample Preparation

The 10 mM stock solutions of SMCFA, including AA, PA, BA, IBA, VA, IVA, and HxA, as well as the internal standard, TFA, were prepared by aliquoting 2.86 µL AA, 3.75 µL PA, 4.62 µL BA, 4.62 µL IBA, 5.44 µL VA, 5.45 µL IVA, 6.31 µL HxA, and 3.85 µL TFA into their respective stock 20-mL glass vials, and diluted with TDI water to the final volume of 5 mL followed by vortex for 1 min. A mixture containing eight acids was prepared by taking an aliquot of 50 µL of each stock acid prepared above in a 1.5-mL centrifuge tube and vortex for 1 min. This standard mixture was filtered with a 0.22-µm

syringe filter and collected into another tube before transferring 100 µL to the CE vial.

The stock solution and the standard mixture were freshly prepared for each experiment.

For example, in some cases, the standard mixture was prepared overnight and stored in

the refrigerator at 4°C, but only analyzed after thawing at room temperature before

transferring to CE vial for analysis. Alternatively, the standard mixture was also

prepared 3-4 hr before CE-IPD analysis.

To prepare the fecal sample solution, the frozen supernatant solution (200 µL

aliquot stored in a freezer at -20°C) was first thawed at room temperature for 10 min.

Next, the diluted supernatant was prepared by aliquoting 30 µL of the supernatant, 18

µL of 10 mM TFA, and 42 µL of TDI water in a 1.5-mL centrifuge tube. This 90 uL fecal

mixture solution was vortexed for 1 min, and the entire solution was transferred to a CE

vial using a micropipette tip set at 90 µL.

3.2.4 Validation of CE-IPD method

The developed CE-IPD method was validated by determining the selectivity,

linearity, limit of detection (LOD), limit of quantitation (LOQ), precision, accuracy,

recovery, robustness, and matrix effect. The calibration curve to determine FA content

in control and drug-treated rat feces (Fig.3.4) was prepared in an adolescent rat fecal

solution, which was previously screened to contain only AA. Five concentration levels of

standard mixture solutions with AA (0.05, 1.70, 3.35, 5.00, and 6.65 mM), PA, BA, IBA,

VA, IVA, and HxA (0.05, 0.20, 0.35, 5.00, and 0.65 mM), with internal standard (TFA, 2

mM) were added into the 5 uL fecal solution of the same adolescent rat lacking other

FAs to construct calibration curve of each acid (see detailed dilution calculation in

Appendix). The same calibration curves were used to determine the trace amount of

endogenous concentration of FA in the fecal matrix obtained from the y-intercept for the curve. The y-intercept values were found to be lower than the LOD for all FAs. The only exception was AA, where the y-intercept value was substantial. The y-intercept value obtained for each plot in the calibration curve for each FA was then added to the spike concentration to generate another set of x values. This set of x values were plotted with the same peak area ratio to determine the unknown concentration of each FA in control and drug-treated rat feces [26]. The LOD and LOQ were calculated from the calibration curve using the formula (three times and ten times the ratio of the standard deviation of the y-intercepts and the slope of the calibration curve, respectively.

To determine the matrix effect, two calibration curves were constructed. To generate the first curve, five concentration levels of standard mixture containing AA (0.5, 1.5, 2.5, 3.5, and 4.5 mM), PA, BA, IBA, VA, IVA, and HxA (0.05, 0.15, 0.25, 0.35, and 0.45 mM) with IS (TFA, 2 mM) was prepared in TDI water. In the second curve, the standard solution was added into the fixed 20 µL of fecal solution. Slopes of the two calibration curves were compared by two methods (see appendix for sample calculations):

1) slope ratio = slope of calibration curve constructed in fecal solution (m_1)/ slope of calibration curve constructed in pure solvent (m_2)

2) slope difference = ($m_1 - m_2$)/ ($m_1 + m_2$)/2 *100%

The slope ratio should be close to 1, and the slope difference should be less than 15% to ascertain that there is no significant matrix effect when the calibration curve is generated in TDI water. Otherwise, matrix-matching calibration has to be considered.

Accuracy, recovery, and precision were determined by spiking experiment at three concentration levels (low = 0.05 mM for all seven SMCFAs, medium = 3.35 mM for AA, 0.35 mM for all other six FAs, high = 6.65 mM for AA, 0.65 mM for all other six FAs) at three different days. The standard mixtures were spiked into the 5 µL fecal solution of the adolescent rat. The calibration curve was used to determine the spike concentration (See appendix for a sample calculation). The accuracy is defined as the percent deviation of the recovered FA when spiked into the fecal solution and was calculated by the following equation as:

Accuracy = (measured concentration of FA in spiked fecal solution – known concentration of spiked FA)÷ known concentration of spiked FA x 100%

The recovery is defined as the percentage of the FA recovered when spiked into the fecal solution and was calculated by the following equation as:

Recovery = (measured concentration of FA in the spiked fecal solution ÷ known concentration of the spiked FA) x 100%

The precision is expressed as the relative standard deviation of peak areas of FAs within three replicate measurements over three different days.

The robustness was evaluated as freeze/ thaw (F/T) stability of the adult fecal supernatant of a controlled rat. The F/T stability was investigated by taking the fecal sample vial (containing 200 uL of supernatant) out of the freezer (-20°C), letting it thaw to room temperature for 10 min, aliquoting 30 uL in a 1.5-mL centrifuge tube, adding 18 uL of 10 mM TFA, and 42 uL TDI water to the same tube. The tube was vortexed for 1 min and immediately transferred to a CE vial to inject for analyzing peak areas of the first F/T cycle. The remaining supernatant solution was stored in the freezer at -20°C for

at least one hour before the above procedure was repeated to prepare for the next F/T cycle. This process was repeated five times, corresponding to five F/T cycles.

3.2.5 CE-UV Instrumentation

The CE separation was performed on Agilent 7100 capillary electrophoresis instrument equipped with a UV detector at a 30 kV power supply. The capillary column was a bare fused silica with an average internal diameter of 75 µm (356 µm OOD), obtained from Polymicro Technologies (Phoenix, AZ). The capillary ends were polished using a polyimide cutter to get smooth flat ends with a total length of 64.5 cm. The column was burnt at 8.5 cm from the capillary outlet to create a UV detection window inserted into the CE alignment interface.

All new capillary columns were rinsed with 1 M NaOH for 30 min, followed by TDI water for 15 min, using high-pressure flush at 2 bar. Pre-conditioning was set as a 5-min flush with prepared buffer solution (8 mM 5'-AMP, 100 mM boric acid, 5 mM α-CD, 7.5 % (v/v) MeOH, adjusted to pH 6.50 using 1 M NaOH). Post-conditioning was set as 2-min flush with TDI water, 2-min 1 M NaOH, and 2-min TDI water, all using high pressure at 2 bar. To convert the negative peaks of IPD as positive peaks, the signal wavelength was set at 320 nm, bandwidth at 10 nm, reference wavelengths at 229 nm, 230 nm, 240 nm, 254 nm, 259 nm, 260 nm, and 274 nm, and reference bandwidth at 60 nm. Agilent MassHunter Workstation Data Acquisition and Agilent MassHunter Qualitative Analysis B.07.00 were used for data analysis and instrument control.

3.3 Results and Discussion

3.3.1 *Optimization of Desiccation Time*

Water content present in stool specimens is a concern for precise measurement of the endogenous concentration of SMCFA in feces. To assess the water content of fecal samples, a desiccation timeline experiment was carried out at six time points, including 2, 4, 6, 8, 10, and 12 hr. The results (Fig.3.1 A-G) indicated that without considering the mass of feces, the SMCFA levels were not significantly different in millimolar concentration (mM, $p > 0.05$). In contrast, a significant change in mass (µmol) of FAs was observed when the mass of feces was taken into account (i.e., µmol/g, $p < 0.001$ for AA and PA, $p < 0.01$ for IBA, BA, IVA, VA, and HxA). As shown, significantly higher µmol/g of each SMCFA was present in fractions, F4-F6 as compared to fractions, F1-F3 all the time ($p < 0.05$), with AA, PA, and BA being the dominant components. The amount of the water loss in fractions F1-F6 is shown in the inset plot H of Fig.3.1. Several trends are evident. First, the loss of water content in the last two fecal fractions, F5 and F6, reached the saturation point around 6 - 8 hr of desiccation. Second, note that different fecal fractions had a slightly different initial water loss, therefore it is expected to have a range in saturation point mentioned above. Nonetheless, to ensure that all fractions reached the saturation point, 8 hr was considered a reasonable estimate for desiccation time before extraction and subsequent analysis.

3.3.2 *Method validation*

The method was validated for selectivity, linearity, the limit of quantitation (LOQ) and limit of detection (LOD), recovery, accuracy and precision, matrix effects, as well as robustness following the guidelines of bioanalytical method from the US FDA [27].

3.3.2.1 Selectivity

According to FDA, the ability of an analytical method to distinguish analyte from everything else that might be in the sample is defined as selectivity or specificity. Thus, selectivity for all seven SMCFAs was investigated by comparing electropherograms of standard solution (Fig, 3.2A) versus extracted blank (control) fecal solution obtained from one of the six fecal fractions (F4, Fig. 3.2B) of the same adult rat feces (spiked with IS). Clearly, the fecal solution is free of interference at the retention time of the FFAs. Additionally, all seven SMCFAs of interest are at least baseline separated from matrix peaks, marked with an asterisk (*) in fecal solution. The RSD values of peak areas of the FAs in the standard mixture as well as in all six fecal fractions did not exceed 11% (inset table shown in Fig.3.2), indicating good repeatability of the method for application in rat feces.

3.3.2.2 Linearity, LOD, and LOQ

The results for linearity, LOD, and LOQ are listed in Table 3.1. Good linearity was attained in all SMCFAs with high correlation coefficients ($R^2 \geq 0.9947$). The linear range was wide enough to cover SMCFA concentrations in the fecal supernatant diluted with IS. The method showed good sensitivity with LOD and LOQ ranging from 0.006 to 0.033 mM and 0.019 to 0.110 mM, respectively. In addition, the LLOD and LLOQ values were calculated at the experimental *S/N* obtained at 0.05 mM of each SMCFA. Therefore, 0.002-0.009 mM and 0.008-0.032 mM are only considered as predicted values obtained from the *S/N* ratio. The only exception was AA that is present in a significant amount in adolescent rat fecal solution.

3.3.2.3 Matrix Effect

The matrix effect was investigated through the slopes of the two calibration curves constructed in fecal solution and in TDI water. The slope ratio of 1 [28] or the slope difference of less than 15% [29] suggests no matrix effect. Our result in Table 3.1 (columns 9 and 10) indicates the number to be in the range of 1.11 to 1.37 for slope ratio and more than 15% for slope difference in most cases. This clearly shows that there is a significant matrix effect. It was reported in the literature that a matrix-matching calibration curve, which could be generated if the blank matrix is similar to the unknown, could provide bias-free analytical results as every sample is assumed to be affected to the same extent [30]. Therefore, to assure method's accuracy, the calibration curves were made by spiking the standard in a fecal sample of one adolescent control rat previously screened to contain no significant FAs. Using the slope and y-intercept, the unknown endogenous concentrations of SMCFA in ten control adults and ten adolescent rats, as well as rats undergoing antibiotic and cocaine treatment for bacterial depletion, consequently decreasing SMCFA in the fecal sample, was measured.

3.3.2.4 Recovery, Accuracy, and Precision

Recovery, accuracy, and precision were assessed by spiking the standard FA mixture at three concentration levels in the fecal solution of an adolescent rat. The results are summarized in Table 3.2. According to FDA guidelines, the percent recovery range should be within ±20% and the percent deviation less than 20%. The intra- and inter-day recovery of all SMCFAs ranged from 87 to 115% at all spike concentration levels, except for HxA and IBA that showed somewhat lower recovery 77 – 81% at low spike concentration. The intra and inter-day accuracy showed less than 15% deviation

at all three concentration levels for all SMCFAs except for the same two FAs mentioned above. The precision was determined through the RSD value of peak area of the FA, resulting in intra-day RSD less than 9% and inter-day RSD less than 14%. Overall, the proposed CE-IPD method demonstrated good recovery, high accuracy, and repeatability for SMCFA analysis in feces.

3.3.2.5 Robustness

As defined by the FDA, robustness measures the bioanalytical assay in which the biological sample's integrity remains unchanged upon minor variations of testing conditions [25]. A freeze/ thaw (F/T) cycle could be considered one example of robustness testing. It involves the procedure in which the temperature is allowed to fluctuate from above freezing to below freezing, then finally return to above freezing. This deliberate change is considered as one F/T cycle. Optimal storage to compare a short and long period for the stability of the extracted fecal solutions remains to be determined. In this study, we investigated the potential effect of a total of five F/T cycles and short-term storage on the concentration of fecal SMCFA.

Two different fecal samples from the different adult rats after their collection and subsequent extraction were subjected to baseline measurement and then stored for eight weeks apart (4 and 12 weeks, respectively) in the freezer -20°C. Each sample was subjected to five F/T cycles. After the sample thawing, fecal solutions are simultaneously prepared (as described in section 3.2.4) and injected in triplicate for peak area analysis. The stability results measured as percent relative error in peak area ratio of FA/IS are compiled in Table 3.3. For the four-week-old supernatant sample, there was a continuous decrease in the peak area ratio of FA/ IS from 21% to 47% up to

the fourth F/T cycle. However, in the fifth cycle, the peak area ratio was increased

compared to the fourth one. On the other hand, for the 12-week-old sample, a

continuous decrease in peak area ratio of FA/ IS was observed up to the third F/T cycle,

then an ascending change in peak area ratio was noted in the fourth and fifth cycles.

The erratic trend of the 12-week old sample might be due to the faster decomposition of

FAs in the completely aqueous supernatant. Nonetheless, our results suggested the

fecal supernatant should be measured only after one F/T cycle because freeze-thawing

the supernatant more than once can create % relative error of $\geq$20%, which is higher

than the acceptable limits of ±15%. We plan to study using a binary solvent mixture of

water with ethanol or propanol in the feces during the extraction process to improve

both the recovery and long-term stability of SMCFA in feces.

3.3.3 Application of CE-IPD method

3.3.3.1 Determination of endogenous concentration of SMCFA in adult and

adolescent rats feces

The validated CE-IPD method was applied to analyze SMCFA in fecal samples

of rats of different ages (adult and adolescent) and drug treatments (antibiotic and

cocaine). In the preliminary work (chapter two), it was found that not as many SMCFA

peaks were identified in the fecal sample from an adolescent rat than an adult rat.

Twenty rats were divided into two groups, one adult group, and another adolescent

group, to extend the work. Therefore, ten animals per group were tested. The results in

Table S3.1 and Table S3.2 list the mean endogenous amount (µmol/g) of SMCFAs

quantitatively measured (using a calibration curve) in ten adult and adolescent rat feces.

The values for adult rats measured in this work reported in Table S3.1 are in good

agreement with literature values, i.e., AA (60-310 µmol/g feces), PA (8-25 µmol/g feces), and BA (8-30 µmol/g feces) [31].

The pie charts in Fig.3.3 (A-B) demonstrate several exciting trends on the relative proportion of seven SMCFAs in fecal samples from adolescent and adult rats. First, in both groups, AA was the most dominant acid (80.4% and 75.1%, respectively), followed by BA, PA, and VA. Second, the branched-chain FAs (IBA and IVA) and MCFA (e.g., HxA) were also found but in meager amounts. For example, IBA, IVA, and HXA levels were 30-200 fold lower than AA in the adult group and even much lower (330-660 fold) in the adolescent group. Noticeably, the standard deviations of the fecal FA concentrations in the adolescent group were substantially higher compared to only a slight variation in the adult group. This finding could imply that the production of SMCFA correlates with the developmental stages of the animals. The adolescent rats at their puberty might produce SMCFA at different levels depending on their maturation. In contrast, the production of SMCFA could get stabilized when the animals reach the adult stage. Finally, the total abundance calculated as the sum of the individual concentration of seven SMCFAs in adult rats was markedly higher (1,103 µmol/g feces) than in adolescent rats (822 µmol/g feces).

3.3.3.2 *Effect of antibiotics and cocaine treatment on SMCFA concentration in rats feces*

The fecal level of SMCFA in adult rats with different drug treatments, including antibiotic and cocaine, was investigated compared to control adult rats (drug-naïve). The result reveals a pronounced reduction of fecal FA in the antibiotic group versus the control group (Fig.3.4). Fecal AA (83±16 µmol/g) and PA (7±1 µmol/g) decreased 96%

in concentration (3.4±0.8 µmol/g and 0.3±0.6 µmol/g, respectively), whereas other straight and branched-chain fecal FAs were disrupted entirely (i.e., no peak was detected). Our result was in line with previous studies on the adverse effect of antibiotic treatment on the fecal concentration of SMCFA [10, 32, 33]. However, the degree of disruption appears to be more severe in our case. Perhaps, factors like types of antibiotics tested, dosage, animals' body weights, and diets might play a role in the outcome. On the other hand, cocaine administration did not suppress the fecal FA level as much as the antibiotic treatments. In particular, cocaine mostly lowered the concentration of HxA (p-value < 0.01), BA, and AA (p values < 0.001) but not significantly reduced VA, IVA, IBA, and PA concentrations (Fig.3.4). A recent study by Chivero et al. suggested that cocaine can disrupt the microbiota and compromise gut barrier integrity [17]. Since SMCFAs are primary products of gut microbiota, an alteration in the abundance of each FA metabolite from our result seemed to align with their findings. Moreover, in another study, it was reported that a change in acetate: propionate ratio where the proportion of propionate significantly increases could lead to a reduction of lipogenesis [34]. Besides, chronic cocaine use is well-known associated with weight loss and malnourishment. Thereby, our results on the proportional change of AA and PA amounts in cocaine-treated rats fortify the hypothesis of the cocaine's influence on lipid metabolism.

3.4 Conclusions

A quantitative CE-IPD method was validated for analysis of fecal SMCFA levels in rats and applied to determine the endogenous amount of SMCFA in adult and adolescent rats as well as to investigate the influences of antibiotic and cocaine

treatments on rats. In addition to method validation, the optimization of the desiccation time provided dried feces samples for accurate quantitation. Moreover, desiccation is a cost-effective water removal method compared with lyophilization. The CE-IPD method showed good linearity ($R^2 \geq 0.995$) with LOD 0.006 to 0.033 mM and LOQ 0.019 to 0.110 mM. Due to higher *S/N* ratio, the predicted LOD and LOQ can be lowered in the range of 0.002-0.009 mM and 0.008-0.032 mM, respectively. Satisfactory recovery (87-115%), high accuracy (deviation less than 15%), and excellent precision (RSD < 14% at all three concentration levels) were also demonstrated. Remarkably, the matrix effect was accounted for when the calibration curve was constructed in the fecal solution, which assured the method accuracy. The supernatant stability was also evaluated to warrant the robustness of the quantitative analysis. The results suggest that the fecal samples should be freeze-thawed only once (if stored at -20 ^{0}C for four weeks or longer) to assure the reliability of the collected peak areas from CE runs.

The validated CE-IPD method was successfully applied to quantify SMCFA concentration in fecal samples of adult and adolescent rats as well as antibiotic and cocaine intake rats. The results revealed significant differences in the abundance of SMCFA in the adult versus adolescent rats, indicating the influence of the developmental stages in the production of SMCFA. Furthermore, both antibiotic and cocaine treatment demonstrated depletion in SMCFA concentration in rat feces. The antibiotic intake rats experienced a more severe reduction in fecal FA concentration, whereas cocaine intake rats underwent the proportional change of fecal FA concentration. Overall, this work is believed to provide profound insights to evaluate the effects of various drug and pain medication treatments in clinical trials.
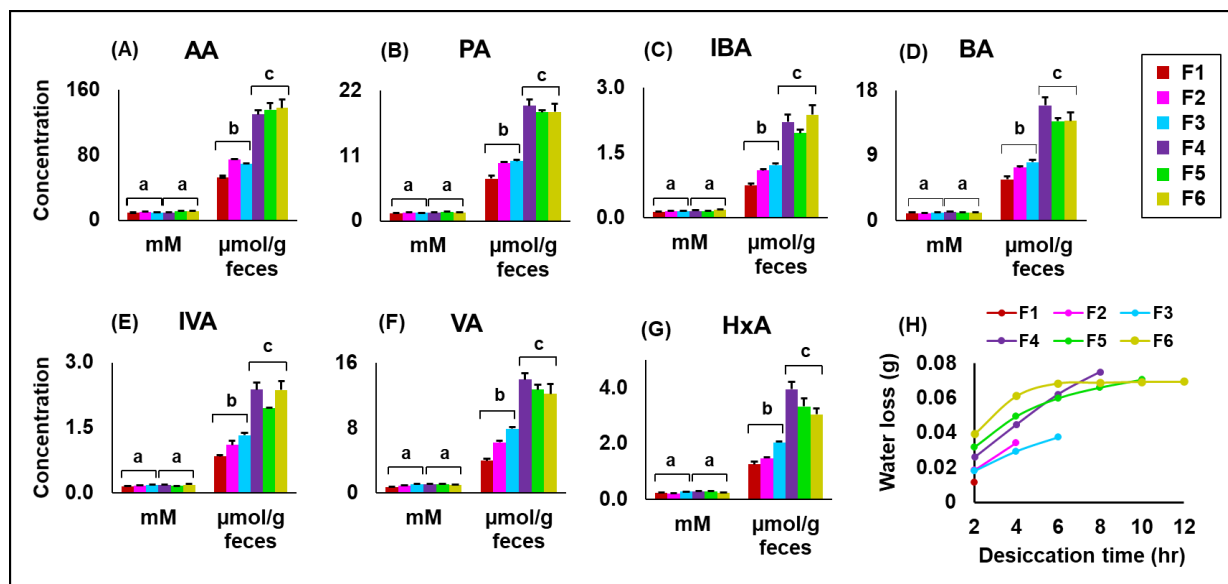
Figure 3.1 Effect of desiccation time on the concentration of SMCFA (A – G) in adult rat feces. Six fecal fractions were collected at different desiccation times including 2, 4, 6, 8,10, and 12 hr. The inset plot (H) indicates the range of water loss measured after every two hour for various fractions. Different letters mean significantly different (p < 0.01) from each other (p values were derived from two-tailed Student t-test).

Intra-sample repeatability (% RSD, n= 3) of peak areas							
	HxA	VA	IVA	BA	IBA	PA	AA
Standard mixture	1	4	2	2	2	2	5
F1 (2hr)	6	4	4	5	3	4	1
F2 (4hr)	6	8	11	4	7	5	4
F3 (6hr)	5	2	5	6	5	5	4
F4 (8hr)	10	5	7	10	9	9	8
F5 (10hr)	3	3	7	5	4	8	2
F6 (12hr)	4	4	4	3	5	3	1
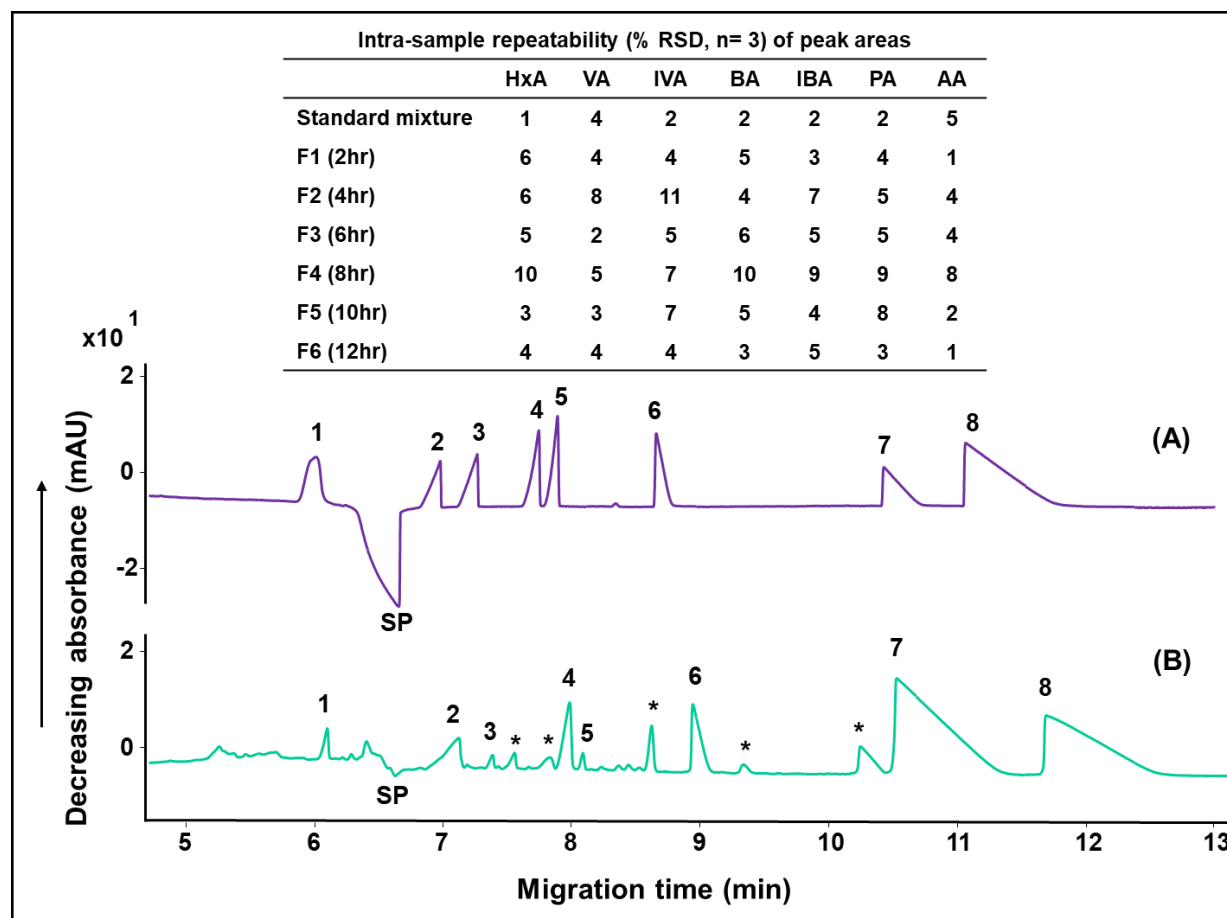
Figure 3.2 Electropherogram of SMCFA in (A) standard mixture and (B) fecal solution (F4 as a representative). The CE-IPD condition as follow: bare fused silica capillary, 75 µm i.d., 56 cm effective length; 100 mM borate buffer containing 8 mM adenosine-5'-monophosphate (5'-AMP), 5 mM alpha-cyclodextrin (α-CD), pH 6.50, 7.5% (v/v) MeOH; injection size 5 mbar 50 s; applied voltage 30 kV (15 µA); UV detection: signal λ at 320 nm, reference λ at 260 nm, bandwidth (10 nm). The arrow indicates the direction of decreasing absorbance. Peak identification: 1. hexanoic acid (HxA), 2. valeric acid (VA), 3. isovaleric acid (IVA), 4. butyric acid (BA), 5. isobutyric acid (IBA), 6. propionic acid (PA), 7. acetic acid (AA), 8. trifluoroacetic acid (internal standard, IS) and system peak (SP). Asterisk-marked are unknown peaks in the fecal solution. The inset table shows the intra-sample repeatability of SMCFA peak areas in standard mixture and in six fractions of adult rat feces corresponding to six desiccation time points.
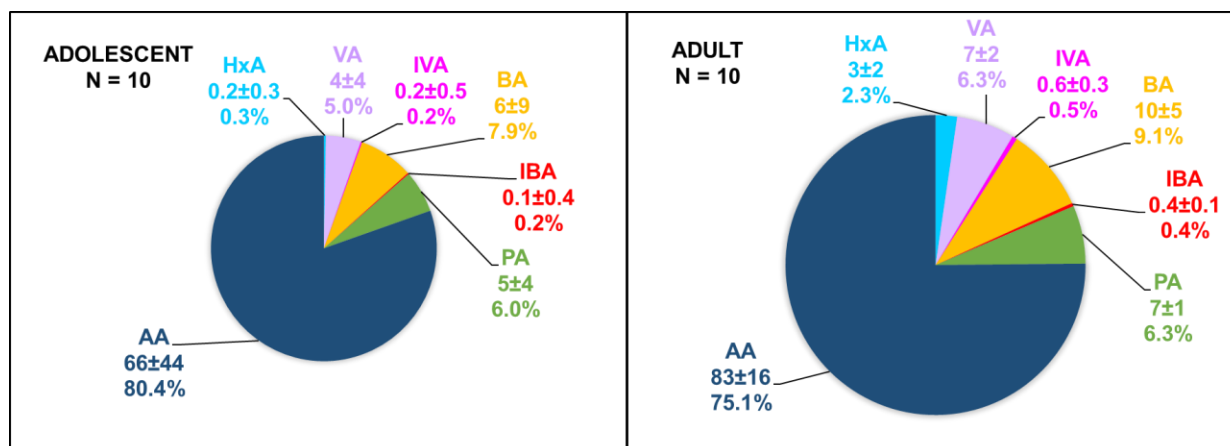
Figure 3.3 Fecal SMCFA concentration in adolescent versus adult rats. The concentration values are in µmol/g feces with standard deviations (n = 10). The percentages are mean relative proportion of seven SMCFAs in the rat feces. The size of each pie chart is an illustration for the difference in the total abundance of fecal SMCFAs in each group.
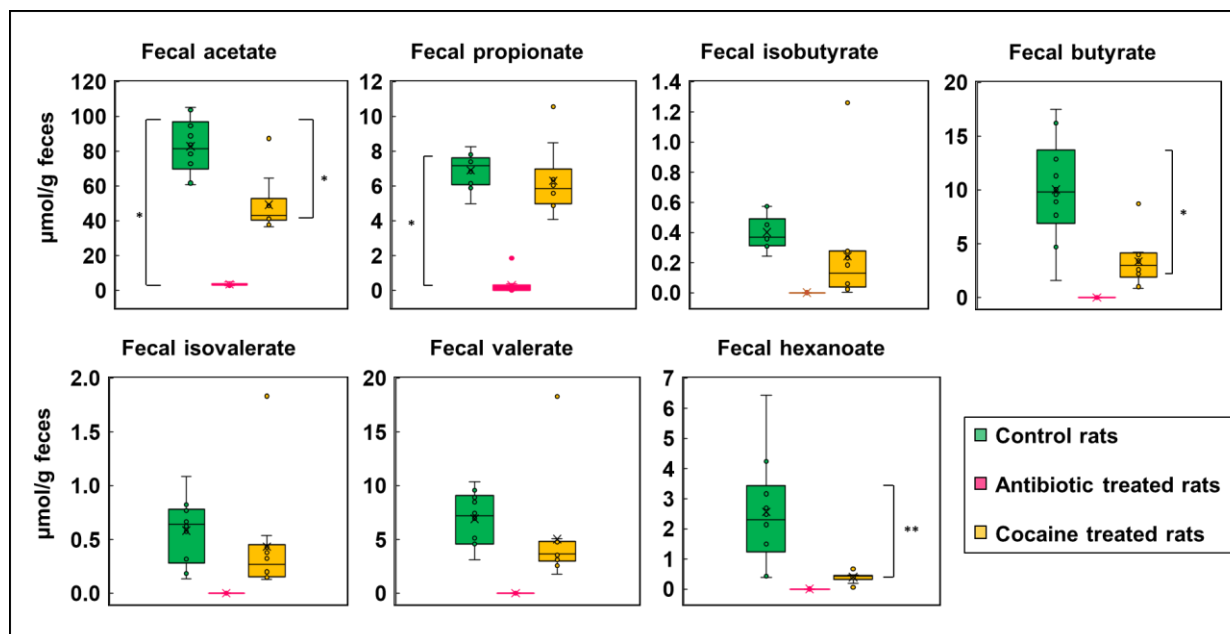
Figure 3.4 A comparison of fecal SMCFA concentration (µmol/g feces) in control, antibiotic and cocaine treated rats. Asterisks indicate statistically significant differences (* $p < 0.001$, ** $p < 0.01$).

Table 3.1 Linearity, limit of detection (LOD), limit of quantitation (LOQ), and matrix effect for quantitative analysis of SMCFA in rat feces using CE-IPD method

FA	Calibration curve[a]	R^2	Linear range (mM)	LOD[b] (mM)	LOQ[b] (mM)	LLOD[c] (mM)	LLOQ[c] (mM)	Matrix effect	
								Slope ratio	Slope difference (%)
AA	y = 0.4757x + 0.0002	0.9999	0.05-6.65	0.033	0.110	_[d]	_[d]	1.15	14
PA	y = 0.4884x + 0.00006	0.9997	0.05-0.65	0.006	0.019	0.002	0.008	1.11	11
IBA	y = 0.415x + 0.0006	0.9962	0.05-0.65	0.022	0.073	0.005	0.018	1.21	19
BA	y = 0.4217x + 0.00009	0.9995	0.05-0.65	0.008	0.027	0.009	0.032	1.27	24
IVA	y = 0.3697x + 0.0002	0.9982	0.05-0.65	0.015	0.051	0.007	0.015	1.31	27
VA	y = 0.369x + 0.00009	0.9992	0.05-0.65	0.010	0.033	0.007	0.025	1.37	31
HxA	y = 0.5432x + 0.0011	0.9947	0.05-0.65	0.026	0.087	0.007	0.024	1.20	18

[a] calibration curve was constructed in fecal matrix
[b] LOD = 3 x σ/m, LOQ = 10 x σ/m where σ is standard deviation of y-intercept and m is slope of calibration curve
[c] LLOD and LLOQ were calculated from experimental *S/N* ratio
[d] LLOD and LLOQ for AA cannot be calculated due to the presence of significant amount of AA in fecal matrix

Table 3.2 Recovery, accuracy, and precision for quantitative analysis of SMCFA in rat feces using CE-IPD method

| FA	Spike level (mM)	Recovery (%)		Accuracy (% Deviation)		Precision (% RSD)	
		Intra-day[a]	Inter-day[b]	Intra-day[a]	Inter-day[b]	Intra-day[a]	Inter-day[b]
AA	0.05	115	104	15	8	6	2
	0.35	102	101	2	2	3	10
	0.65	99	100	0.7	0.7	4	2
PA	0.05	97	93	3	7	7	7
	0.35	101	101	1	1	2	10
	0.65	97	98	3	2	3	5
IBA	0.05	77	81	23	19	9	7
	0.35	105	104	5	4	3	10
	0.65	96	97	4	3	2	4
BA	0.05	87	89	13	11	8	8
	0.35	102	102	2	2	5	6
	0.65	99	99	1	1	2	2
IVA	0.05	105	97	5	7	9	4
	0.35	100	103	0.5	3	4	11
	0.65	98	99	2	0.9	4	3
VA	0.05	94	90	6	12	9	10
	0.35	100	101	0.5	2	6	11
	0.65	97	100	3	1	4	6
HxA	0.05	79	70	21	30	8	10
	3.35	106	108	6	8	0.4	14
	6.65	97	97	3	3	4	7

[a]Intra-day n = 3, [b]Inter-day n = 9

Table 3.3 Percent relative error in peak area ratio of fatty acid and internal standard in comparison between samples after 2nd, 3rd, 4th, and 5th freeze/thaw cycle and sample freeze-thawed once

	Percent relative error[†] (%) in peak area ratio FA/IS						
4-week-old fecal supernatant							
Number of F/T cycles	HxA	VA[‡]	IVA[‡]	BA	IBA	PA	AA
2	-23 ±4	-21 ±1	-28 ±1	-24 ±3	-22 ±5	-23 ±3	-23 ±6
3	-24 ±2	-22 ±2	-32 ±3	-25.7 ±0.6	-26 ±1	-24.6 ±0.4	-24 ±1
4	-46 ±1	-39.3 ±0.6	-51 ±2	-47 ±1	-44 ±2	-45 ±1	-42.1 ±0.9
5	-28 ±2	--	--	-32 ±2	-29 ±3	-30 ±1	-27 ±1
12-week-old fecal supernatant							
Number of F/T cycles	HxA	VA	IVA	BA	IBA	PA	AA
2	-2 ±3	-2 ±1	-4 ±5	-1.1 ±0.7	-2 ±3	2 ±3	3.2 ±0.6
3	-29 ±7	-21 ±4	-25 ±3	-21.4 ±0.8	-25 ±5	-20 ±2	-19 ±1
4	21 ±4	11 ±10	16 ±5	17 ±1	14 ±4	18 ±4	17 ±6
5	45 ±5	39 ±8	33 ±6	38 ±2	29 ±5	29 ±3	20 ±3

[†] Percent relative error =((peak area ratio from the nth F/T cycle - peak area ratio from the 1st F/T cycle)/ peak area ratio from the 1st F/T cycle)* 100, where n = 2, 3, 4, 5. Negative value means decrease in peak area ratio, whereas positive value means increase in peak area ratio.

[‡] VA and IVA peaks in the 5th F/T cycle sample were undetermined due to being considerably diminished.

4   FUTURE DIRECTIONS

The developed assay in this work has shown strong potential in routine analysis of SMCFA in feces. For future applications in basic and clinical research, this assay can be further improved. At least three frontiers are worth considering. First, recovery and robustness could be improved. Different types of organic solvents such as methanol, ethanol, propanol, and acetonitrile can be explored to obtain a higher percent recovery in the extraction of SMCFA from feces. The long-term stability of fecal supernatant can be examined to extend the robustness assessment. Second, the finding on the larger variation in fecal SMCFA levels, especially branched-chain and medium-chain FAs, in an adolescent group than in an adult group, suggests a future study on narrower developmental stages including early adolescent/ adult, mid adolescent/ adult, and late adolescent/ adult. Therefore, it would be exciting to learn at what stage the production of SMCFA starts to grow drastically. Moreover, from the findings on antibiotic and cocaine treatment influences, an investigation on the recovery period (post-drug administration) is suggested. Third, various types of antibiotics could govern different mechanisms in the functioning of gut microbiota. The results obtained for the antibiotic study were from the rats that were treated with a combination of three antibiotics, including neomycin, bacitracin, and ampicillin. A survey on the impact of the individual antibiotic mentioned above, or exploring a new generation of antibiotics can be performed to gain more insights on SMCFA levels after treatment with different types antibiotics.

APPENDICES

Appendix A

Table S2.1 Effect of alpha-cyclodextrin concentration on migration time (min)

	n=3	OA[†]	HpA	HxA[‡]	VA	IVA	BA	IBA	PA	AA
0 mM α-CD	Average	-	8.3	8.7	9.1	9.2	9.8	9.8	11.0	14.2
	St. Dev	-	0.2	0.2	0.2	0.2	0.2	0.2	0.3	0.5
	% RSD	-	2	2	2	2	3	3	3	4
3 mM α-CD	Average	5.8	6.4	-	8.4	8.7	9.4	9.5	10.6	13.6
	St. Dev	0.1	0.1	-	0.2	0.2	0.3	0.3	0.3	0.5
	% RSD	2	2	-	2	3	3	3	3	4
4 mM α-CD	Average	5.9	6.5	7.5	8.7	9.2	9.9	10.1	11.4	15
	St. Dev	0.1	0.2	0.2	0.3	0.3	0.4	0.4	0.5	1
	% RSD	2	3	3	3	4	4	4	5	7
5 mM α-CD	Average	5.5	5.9	6.6	7.8	8.2	8.8	9.0	10.0	12.6
	St. Dev	0.1	0.1	0.2	0.2	0.2	0.2	0.2	0.3	0.4
	% RSD	2	2	2	2	3	3	3	3	3
7 mM α-CD	Average	5.6	6.0	6.7	8.1	8.7	9.4	10	11	14
	St. Dev	0.3	0.4	0.5	0.7	0.8	0.9	1	1	2
	% RSD	6	6	7	9	9	10	10	12	16

[†] OA peak was lost into SP profile without α-CD
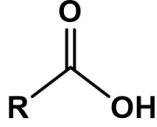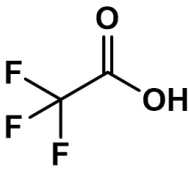[‡] HxA peak was lost into SP profile with 3 mM α-CD

Table S2.2a Effect of 5'-AMP concentration on resolution (*Rs*) and selectivity (*α*)

		n=3	OA/HpA	HpA/HxA	HxA/SP	SP/VA	VA/IVA	IVA/BA	BA/IBA	IBA/PA	PA/AA
7 mM 5'-AMP	*Rs*	Average	2.33	2.5	1.5	1.3	1.76	3.03	1.43	5.6	6.6
		St. Dev	0.06	0.1	0.1	0.1	0.08	0.08	0.04	0.2	0.2
		% RSD	2	4	6	8	5	3	3	4	3
	α	Average	1.339	1.384	1.23	1.13	1.105	1.135	1.038	1.181	1.394
		St. Dev	0.005	0.001	0.01	0.01	0.004	0.003	0.001	0.004	0.009
		% RSD	0.4	0.1	1	0.9	0.3	0.2	0.1	0.4	0.6
8 mM 5'-AMP	*Rs*	Average	2.6	3.2	1.8	1.7	2.0	3.5	1.61	6.5	7.4
		St. Dev	0.2	0.2	0.2	0.1	0.2	0.2	0.05	0.4	0.5
		% RSD	6	7	14	7.0	8	6	3	7	7
	α	Average	1.346	1.388	1.219	1.164	1.114	1.148	1.040	1.204	1.45
		St. Dev	0.003	0.005	0.009	0.006	0.004	0.006	0.001	0.007	0.02
		% RSD	0.2	0.3	0.7	0.5	0.4	0.5	0.1	0.6	1
9 mM 5'-AMP	*Rs*	Average	3.0	3.9	2.4	2.0	2.17	4.1	1.73	7.7	9.4
		St. Dev	0.1	0.2	0.3	0.1	0.09	0.2	0.07	0.3	0.5
		% RSD	4	5	11	5	4	5	4	4	5
	α	Average	1.37	1.41	1.24	1.171	1.120	1.171	1.046	1.243	1.547
		St. Dev	0.02	0.02	0.01	0.007	0.003	0.005	0.001	0.008	0.008
		% RSD	2	1	0.9	0.6	0.3	0.4	0.09	0.6	0.5

Table S2.2b Effect of 5'-AMP concentration on *S/N* ratio

n=3		OA	HpA	HxA	VA	IVA	BA	IBA	PA	AA
7 mM	Average	920	1300	1200	680	790	870	890	960	1100
5'-AMP	St. Dev	72	122	63	22	62	70	72	100	93
	% RSD	8	10	5	3	8	8	8	10	9
8 mM	Average	730	1000	970	590	670	720	740	840	990
5'-AMP	St. Dev	58	93	63	42	35	48	54	38	55
	% RSD	8	9	7	7	5	7	7	5	6
9 mM	Average	490	700	650	400	450	520	530	610	740
5-AMP	St. Dev	18	26	52	20	16	11	10	22	34
	% RSD	4	4	8	5	4	2	2	4	5

Number of carbon atoms	IUPAC name	Common name	Formula	pKa*
2	Acetic acid	Acetic acid	CH_3COOH	4.75
3	Propanoic acid	Propionic acid	CH_3CH_2COOH	4.88
4	Butanoic acid	Butyric acid	$CH_3CH_2CH_2COOH$	4.82
4	2-Methylpropanoic acid	Isobutyric acid	$(CH_3)_2CHCOOH$	4.84
5	Pentanoic acid	Valeric acid	$CH_3(CH_2)_3COOH$	4.84
5	3-Methylbutanoic acid	Isovaleric acid	$(CH_3)_2CHCH_2COOH$	4.77
6	Hexanoic acid	Caproic acid	$CH_3(CH_2)_4COOH$	4.88
7	Heptanoic acid	Enanthic acid	$CH_3(CH_2)_5COOH$	4.89
8	Octanoic acid	Caprylic acid	$CH_3(CH_2)_6COOH$	4.89

Short and medium chain fatty acids (R: carbon chain length)

Trifuoroacetic acid (TFA) (Internal standard, IS)

* Values taken from PubChem, https://pubmed.ncbi.nlm.nih.gov/

Figure S2.1 Nomenclature, *pKa* values, and chemical structure of SMCFA and internal standard.
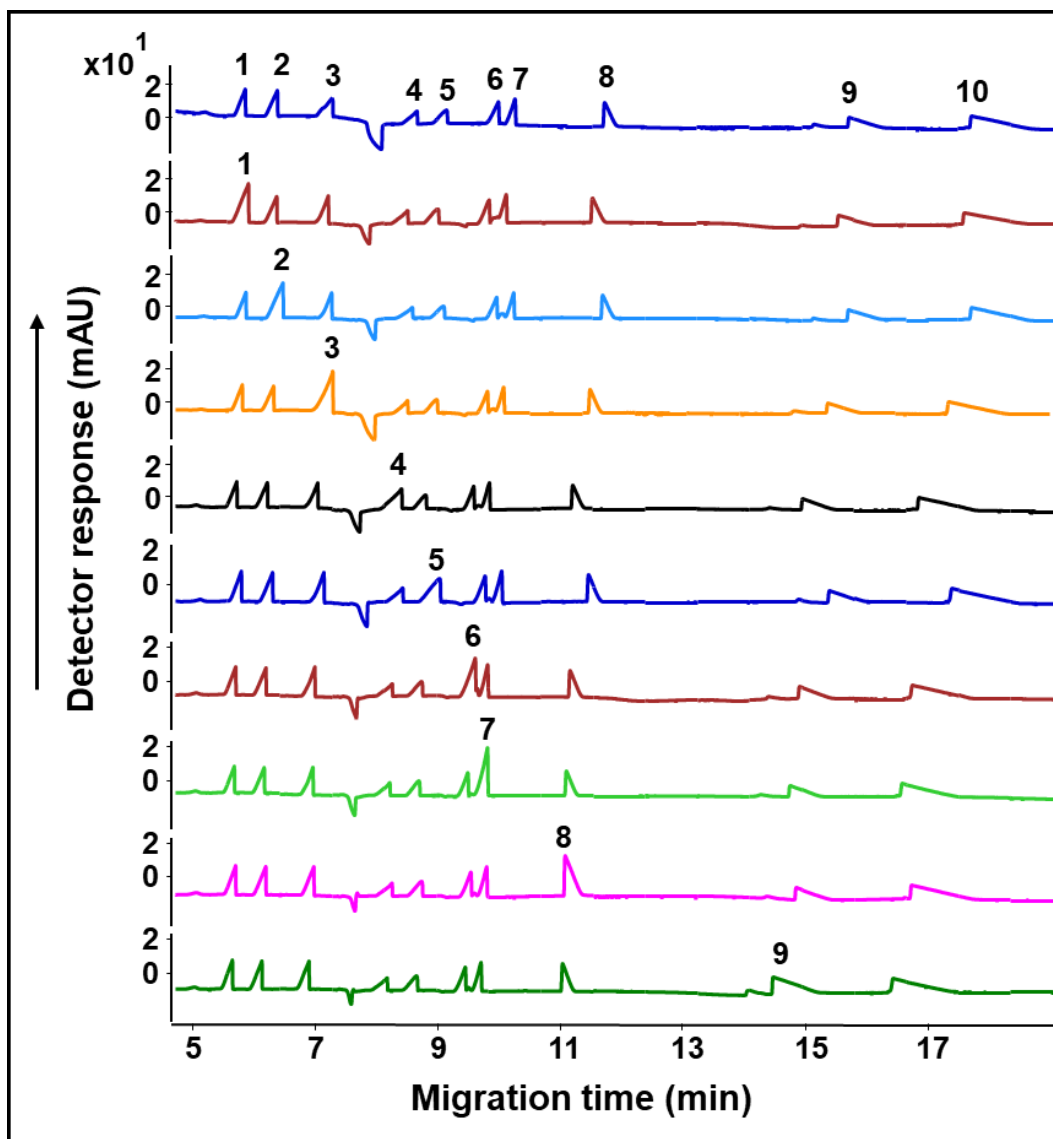
Figure S2.2 Verification of elution order of SMCFA by automated spiking method using Agilent MassHunter Workstation Data Acquisition software. The CE separation conditions are identical to Fig.2.1B. Peak identification is the same as Fig. 1.The top electropherogram represent a mixture of nine SMCFA at 0.5 mM and 1mM TFA as an internal standard. Each of the subsequent electropherogram is obtained by setting two command lines in the injection tab . The first line was set to inject a standard mixture at an injection size of 5 mbar for 50 s. The second line was set to inject a single standard FA at the same injection size prepared separately at 0.5 mM for individual spiking.
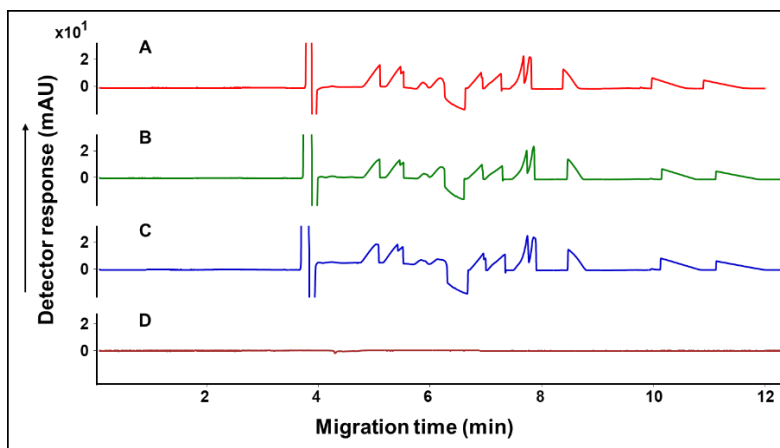
Figure S2.3 Determining the origin of the system peak in IPD running buffer by automated spiking method with following settings (A) injection (5 mbar 50s) of standard mixture only, (B) injection of standard mixture spiked with 50 mM boric acid (both 5 mbar, 50s), (C) injection of standard mixture spiked with 1 mM 5'-AMP in 50 mM boric acid (both 5 mbar, 50s), and (D) injection (5 mbar 50s) of standard mixture only with exclusion of 5'-AMP in running buffer. CE separation conditions are identical to Fig.2.1 except for 3 mM of 5'-AMP in running buffer for electropherograms A-C.
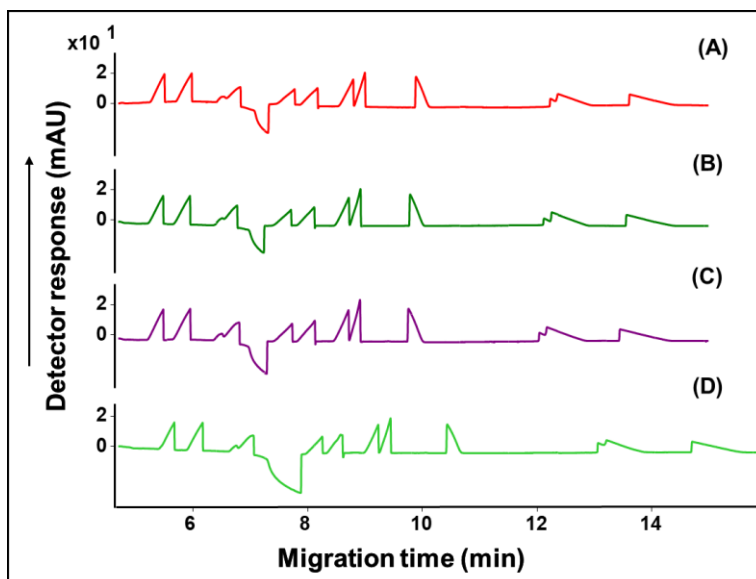
Figure S2.4. Determining the origin of the system peak in IPD running buffer by automated spiking method with following settings: (A) injection of standard mixture only (5 mbar, 50 s (B) injection of standard mixture spiked with H_2O (both set at 5 mbar, 50s in two separate command lines), (C) injection of standard mixture spiked with 1 mM 5'-AMP in H_2O (both set at 5 mbar, 50s in two separate command lines) , and (D) injection of standard mixture spiked with 7 mM 5'-AMP in H_2O (both set at 5 mbar, 50s in two separate command lines) The CE separation conditions are identical to Fig.2.1 except for 5 mM of 5'-AMP in running buffer.
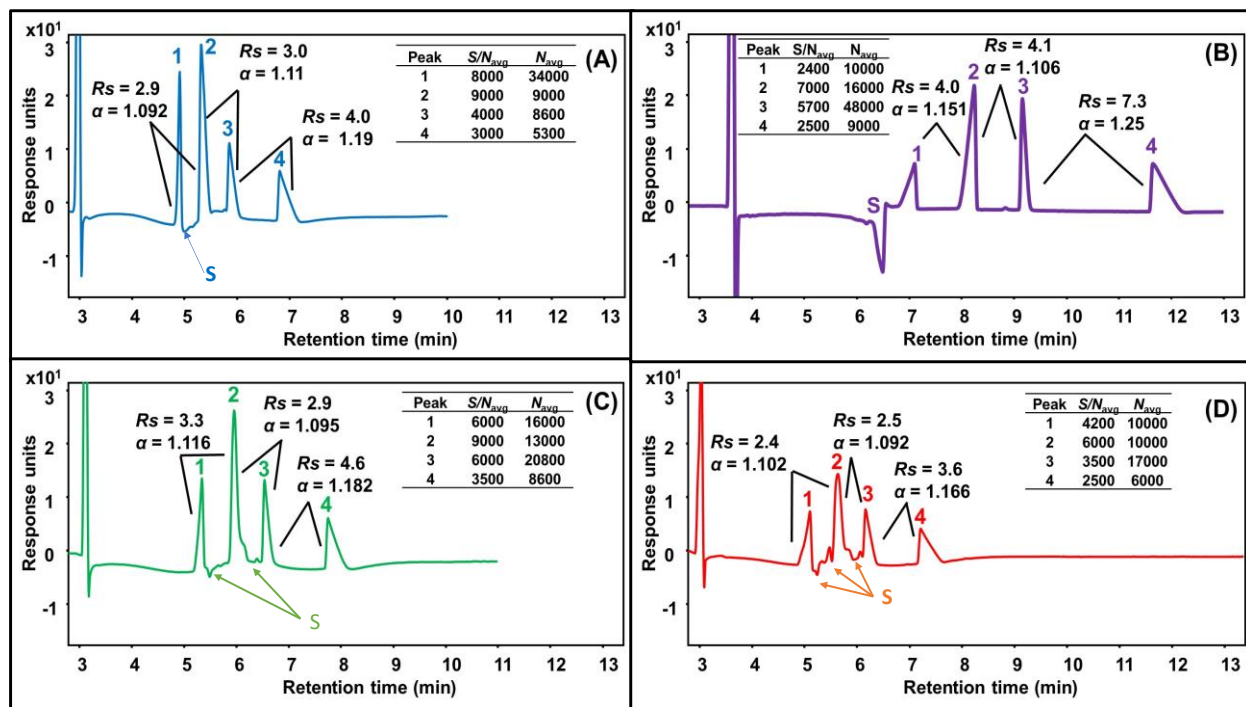
Figure S2.5 Comparison of four IPD reagents for the separation of SCFAs. CE separation conditions are identical to Fig.2.1A except the type of IPD reagent is varied. (A) = parahydroxybenzoic acid (PHBA), B = adenosine 5'-monophospate (5'-AMP), C = nitrobenzoic acid (NBA), D= naphthalene monosulfonate (NMS). Peak identification: 1 = 2-ethylbutyric acid (IS), 2 = butyric acid (BA) and isobutyric acid (IBA), 3 = propionic acid (PA), 4 = acetic acid (AA), S = system peak.
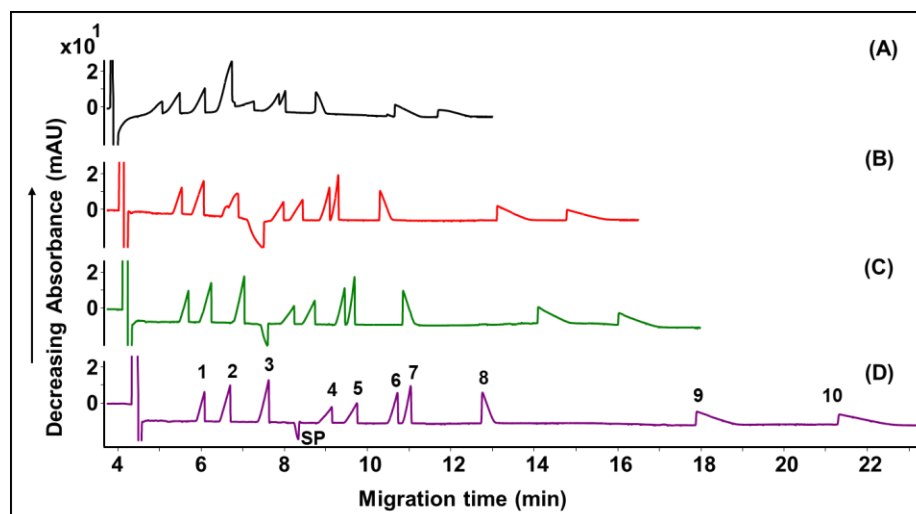
Figure S2.6 Effect of 5'-AMP concentration on the separation of SMCFA using CE-IPD. CE separation conditions are identical to Fig.2.1 except for 7.5% MeOH and varied concentration of 5'-AMP (A) 3 mM, (B) 5 mM, (C) 7 mM, (D) 9 mM. Peak identification is the same as Fig.2.1.
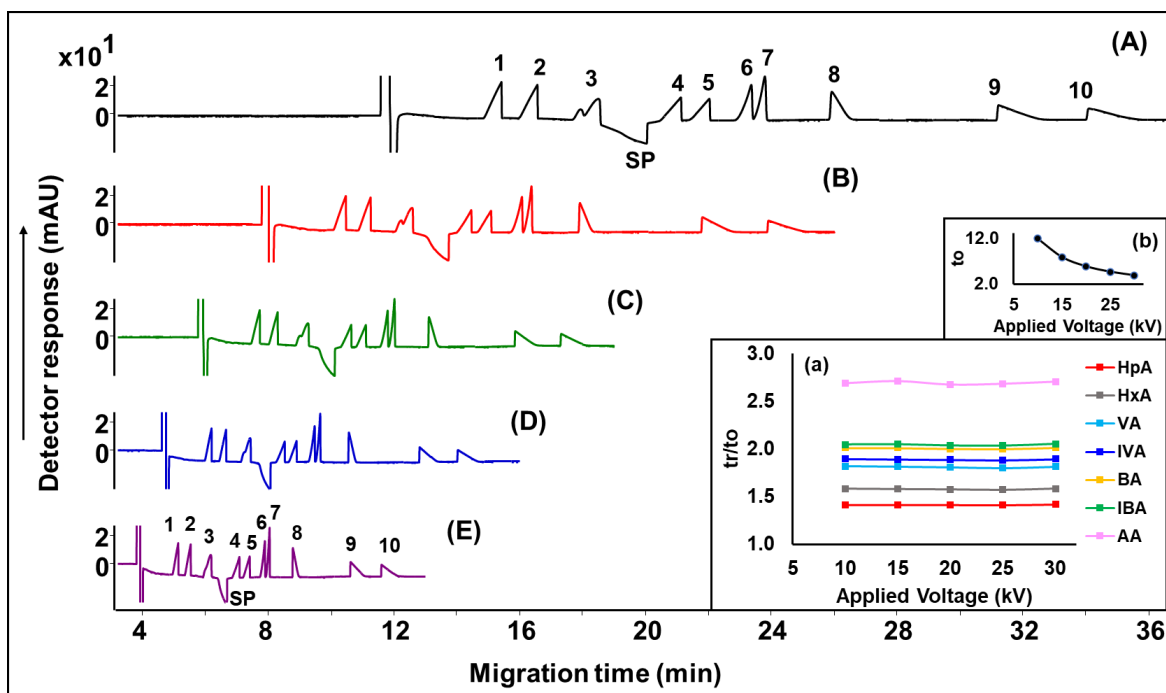
Figure S2.7 Effect of applied voltage on the separation of SMCFA. The CE conditions are identical to Fig.2.1 except for 8 mM 5'-AMP and varied voltage as (A) 10 kV, (B) 15 kV, (C) 20 kV, (D) 25 kV, (E) 30kV. Peak identification is the same as Fig. .1. Inset plots are (a) t_r/t_o and (b) t_o as a function of applied voltage.
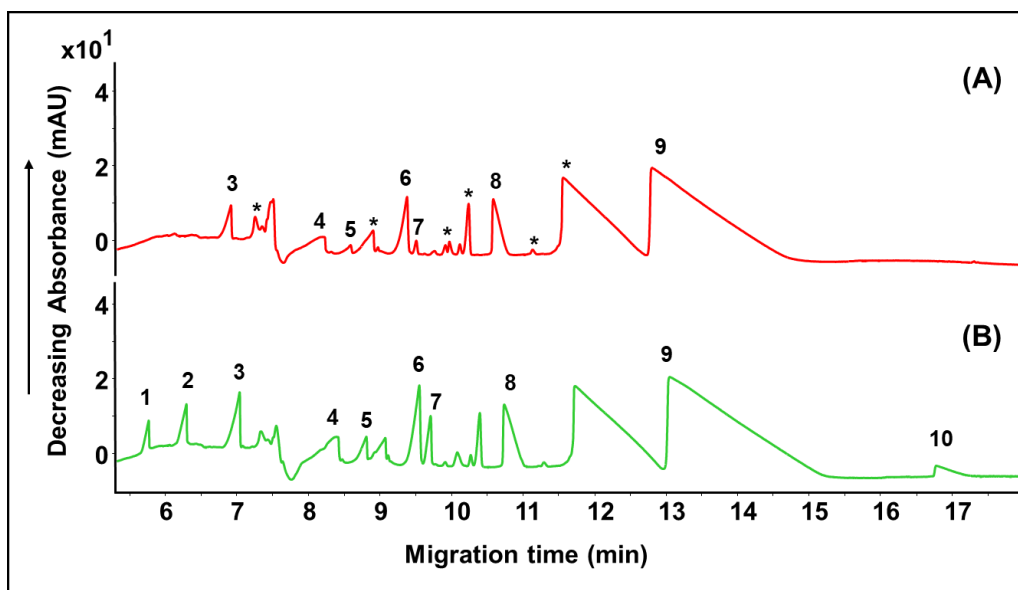
Figure S2.8 Identification of SMCFA in rat fecal sample by automated spiking method: (A) unspiked (B) spiked. CE separation conditions are identical to Fig.2.1 except for 7.5% MeOH and 8 mM 5'-AMP. Peak identification is the same as Fig.2.1. Asterisk-marked peaks are unknown from the matrix.

Appendix B

Table S3.1 Mean endogenous amount (µmol/ g feces) of SMCFA in feces from ten adult control rats.

| Fecal sample	HxA	VA	IVA	BA	IBA	PA	AA
A1	2.2 ±0.2	4.6 ±0.5	0.32 ±0.03	8.9 ±0.2	0.31 ±0.03	7.4 ±0.2	105 ±1
A2	2.7 ±0.06	7.0 ±0.4	0.67 ±0.05	12.9 ±0.5	0.58 ±0.02	6.8 ±0.3	89 ±7
A3	4.23 ±0.07	7.4 ±0.4	0.67 ±0.04	7.7 ±0.3	0.36 ±0.02	6.2 ±0.2	84 ±2
A4	6.4 ±0.2	10.4 ±0.7	1.09 ±0.02	17.5 ±0.6	0.57 ±0.02	7.5 ±0.2	104 ±4
A5	2.13 ±0.03	9.6 ±0.5	0.83 ±0.04	10.07 ±0.09	0.46 ±0.03	5.88 ±0.03	73 ±2
A6	0.38 ±0.01	5.11 ±0.08	0.14 ±0.02	4.72 ±0.08	0.24 ±0.02	7.4 ±0.1	62 ±2
A7	0.42 ±0.05	3.1 ±0.3	0.18 ±0.02	1.58 ±0.04	0.31 ±0.01	8.3 ±0.2	92 ±2
A8	2.7 ±0.1	8.5 ±0.4	0.77 ±0.03	9.6 ±0.3	0.45 ±0.04	4.98 ±0.06	60 ±2
A9	3.2 ±0.2	8.9 ±0.7	0.63 ±0.05	16 ±1	0.37 ±0.04	6.9 ±0.3	79 ±5
A10	1.50 ±0.09	4.6 ±0.2	0.58 ±0.04	11.3 ±0.5	0.37 ±0.03	7.8 ±0.2	79 ±1

Table S3.2 Mean endogenous amount (µmol/ g feces) of SMCFA in feces from ten adolescent control rats.

Fecal sample	HxA	VA	IVA	BA	IBA	PA	AA
P1	ND	1.62 ±0.01	ND	2.00 ±0.03	ND	4.69 ±0.04	35.9 ±0.3
P2	0.285 ±0.008	3.9 ±0.1	ND	2.64 ±0.03	ND	1.58 ±0.09	38.0 ±0.4
P3	0.41 ±0.05	3.1 ±0.3	ND	4.8 ±0.3	ND	3.72 ±0.06	68 ±4
P4	1.1 ±0.1	3.1 ±0.1	ND	11.04 ±0.09	ND	4.37 ±0.07	60 ±2
P5	0.14 ±0.02	3.8 ±0.1	ND	3.56 ±0.09	0.098 ±0.006	2.42 ±0.04	52 ±3
P6	ND	6.9 ±0.2	ND	5.6 ±0.2	0.20 ±0.04	4.67 ±0.06	91 ±1
P7	ND	13.8 ±0.2	1.58 ±0.02	31.1 ±0.7	1.20 ±0.03	15.4 ±0.1	178 ±6
P8	0.26 ±0.04	1.25 ±0.07	ND	ND	ND	4.47 ±0.05	29 ±1
P9	0.22 ±0.04	0.79 ±0.05	ND	ND	ND	4.1 ±0.1	34.3 ±0.7
P10	ND	3.01 ±0.05	ND	3.9 ±0.1	ND	4.30 ±0.03	76 ±3

ND: Not detected

Table S3.3 Sample calculation and preparation of calibration curve constructed in fecal

solution (adolescent rat)

point 1	stock (mM)	final conc (mM)	final vol (uL)	aliquot (uL)
AA	1	0.05	100	5
PA	1	0.05	100	5
IBA	1	0.05	100	5
BA	1	0.05	100	5
IVA	1	0.05	100	5
VA	1	0.05	100	5
HxA	1	0.05	100	5
TFA	10	2	100	20
			FS	5
			H2O	40
point 2	stock (mM)	final conc (mM)	final vol (uL)	aliquot (uL)
AA	10	1.7	100	17
PA	5	0.2	100	4
IBA	5	0.2	100	4
BA	5	0.2	100	4
IVA	5	0.2	100	4
VA	5	0.2	100	4
HxA	5	0.2	100	4
TFA	10	2	100	20
			FS	5
			H2O	34
point 3	stock (mM)	final conc (mM)	final vol (uL)	aliquot (uL)
AA	25	3.35	100	13.4
PA	5	0.35	100	7
IBA	5	0.35	100	7
BA	5	0.35	100	7
IVA	5	0.35	100	7
VA	5	0.35	100	7
HxA	5	0.35	100	7
TFA	10	2	100	20
			FS	5
			H2O	19.6
point 4	stock (mM)	final conc (mM)	final vol (uL)	aliquot (uL)
AA	25	5	100	20
PA	10	0.5	100	5
IBA	10	0.5	100	5
BA	10	0.5	100	5
IVA	10	0.5	100	5
VA	10	0.5	100	5
HxA	10	0.5	100	5
TFA	10	2	100	20
			FS	5
			H2O	25
point 5	stock (mM)	final conc (mM)	final vol (uL)	aliquot (uL)
AA	25	6.65	100	26.6
PA	10	0.65	100	6.5
IBA	10	0.65	100	6.5
BA	10	0.65	100	6.5
IVA	10	0.65	100	6.5
VA	10	0.65	100	6.5
HxA	10	0.65	100	6.5
TFA	10	2	100	20
			FS	5
			H2O	9.4

Sample calculations for LLOD and LLOQ

S/N_{HxA} = 20.950 at 0.05 mM

For LLOD,

Response factor = $S/N \div 3$ = 20.950 ÷ 3 = 6.983

LLOD = Concentration ÷ response factor = 0.05 mM ÷ 6.983 = 0.007 mM

For LLOQ,

Response factor = $S/N \div 10$ = 20.950 ÷ 10 = 2.095

LLOQ = Concentration ÷ response factor = 0.05 mM ÷ 2.095 = 0.024 mM

Sample calculations for slope ratio and slope difference

Calibration curve for HxA

- in fecal solution: y = 1.3874x – 0.0074 → slope m_1 = 1.3874

- in TDI water: y = 1.1552x + 0.0019 → slope m_2 = 1.1552

Slope ratio = $m_1 \div m_2$ = 1.3874 ÷ 1.1552 = 1.2

Slope difference = $(m_1 - m_2) \div [(m_1 + m_2) \div 2]$ x 100% = 18%

Sample calculations for accuracy and recovery

Accuracy and recovery of AA at medium spike level of 3.35 mM

- known spike concentration = 3.35 mM

- measured concentration in spike fecal solution: use calibration curve as follow

Plot 1: y = 2.1022x – 0.3833 where y = spike concentration of AA

x = peak area ratio of AA/IS

$[AA]_{present\ in\ fecal\ solution}$ = y-intercept = 0.3833 mM

Plot 2: y = 2.1022x – 0.000003 where y = $[AA]_{present\ in\ fecal\ solution}$ + $[AA]_{spike}$

x = peak area ratio of AA/IS

[AA]present in fecal solution + [AA]spike = 2.1022 x 1.8023 − 0.000003 = 3.7888 mM

→ [AA]spike = 3.7888 mM − 0.3833 mM = 3.4055 mM

Accuracy (% deviation) = |3.35 mM − 3.4055 mM| ÷ 3.35 mM x 100% = 1.66%

Recovery = 3.4055 mM ÷ 3.35 mM x 100% = 102%

Preparation of stock SMCFA solutions

The stock SMCFA solution was prepared at a concentration of 10 mM in a volume of 5 mL. First, the weight of the acid was calculated using the formula below.

m = molecular weight (g/mol) * molar concentration (mol/L) * volume (L)

Next, the volume needed to make the stock solution was calculated using the density of the acid as below.

v = mass (g) / density (g/mL)

Example calculation:

Acetic acid (m.w. 60.052 g/mol, density 1.05 g/mL)

m = 60.052 g/mol * 10×10^{-3} mol/L * 5×10^{-3} L = 3.0026×10^{-3} g (0.0030 g)

v = 3.0026×10^{-3} g / 1.05 g/mL = 2.8596×10^{-3} mL = 2.86 µL

The volume of 4,997.14 µL H_2O is added to make to the final volume of 5 mL.

REFERENCES

Chapter 1

[1]   Voreades, N., Kozil, A., Weir, T. L., *Front Microbiol.*, 2014, 5, 494.

[2]   Zhu, W., Lin, K., Li, K., Deng, X., Li, C., *Food Funct.*, 2018, 9, 541-551.

[3]   Wan, J., Hu, S., Ni, K., Chang, G., Sun, X., Yu, L., *PLoS ONE,* 2016, 11, e0164894.

[4]   Yousi, F., Kainan, C., Junnan, Z., Chuanxing, X., Lina, F., Bangzhou, Z., Jianlin, R., & Baishan, F., *AMB Express*, 2019, *9*, 69.

[5]   Cook, S. I., Sellin, J. H., *Aliment Pharmacol Ther.*, 1998, 12, 499-507.

[6]   Topping, D. L., Clifton, P. M., *Physiol Rev.*, 2001, 81, 1031-64.

[7]   Kim, Y. S., Tsao, D., Siddiqui, B., Whitehead, J. S., Arnstein, P., Bennett, J., Hicks, J., *Cancer.*, 1980, 45, 1185-92.

[8]   Barnard, J. A., Warwick, G., *Cell Growth Differ.*, 1993, 4, 495-501.

[9]   Bornet, F. R., Brouns, F., Tashiro, Y., Duvillier, V., *Dig Liver Dis.*, 2002, 34, S111-20.

[10]   Katzinger, J., in *Textbook of Natural Medicine* (5th ed.), 2020, 227-235.

[11]   Machate, D. J., Figueiredo, P. S., Marcelino, G., Guimarães, R. d. C. A., Hiane, P. A., Bogo, D., Pinheiro, V. A. Z., Oliveira, L. C. S. d., Pott, A., *Int. J. Mol. Sci.* 2020, *21*, 4093.

[12]   Baltić, B., Starčević, M., Đorđević, J., Mrdović, B., Marković, R., *IOP Conf. Ser.: Earth Environ. Sci.* 2017, 85, 012048.

[13] Van Immerseel, F., De Buck, J., Boyen, F., Bohez, L., Pasmans, F., Volf, J., Sevcik, M., Rychlik, I., Haesebrouck, F., Ducatelle, R., *Applied and environmental microbiology*, 2004, *70*, 3582–3587.

[14] Lemarié, F., Beauchamp, E., Legrand, P., Rioux, V., *Biochimie.*, 2016, 120, 40-8.

[15] https://pubmed.ncbi.nlm.nih.gov/

[16] https://scifinder--n-cas-org.eu1.proxy.openathens.net/

[17] https://clarivate.com/webofsciencegroup/solutions/web-of-science/

[18] https://www.sciencedirect.com/

[19] Weitkunat, K., Schumann, S., Petzke, K. J., Blaut, M., Loh, G., Klaus, S., *J Nutr Biochem.*, 2015, 26, 929-37.

[20] Shen, Q., Tuohy, K. M., Gibson, G. R., Ward, R. E., *Lett Appl Microbiol.*, 2011, 52, 337-43.

[21] Pham, T., Teoh, K. T., Savary, B. J., Chen, M. H., McClung, A., Lee, S. O., *Nutrients*, 2017, *9*, 1237.

[22] Hu, J. L., Nie, S. P., Min, F. F., Xie, M. Y., *J Agric Food Chem.*, 2012, 60, 11525-32.

[23] Tao, J., Duan, J., Jiang, S., Guo, J., Qian, Y., Qian, D., *J. Chromatogr. B,* 2016, 1029–1030, 88-94.

[24] Zhao, X., Jiang, Z., Yang, F., Wang, Y., Gao, X., Wang, Y., Chai, X., Pan, G., Zhu, Y., *PLoS ONE*, 2016, 11, e0167032.

[25] Wang, L. L., Guo, H. H., Huang, S., Feng, C. L., Han, Y. X., Jiang, J. D., *J Chromatogr B Analyt Technol Biomed Life Sci.,* 2017, 1057, 70-80.

[26] Kim, H., Kwon, J., Choi, S. Y., Ahn, Y. G., *J Anal Sci Technol,* 2019, 10, 28.

[27] Zheng, X., Qiu, Y., Zhong, W., Baxter, S., Su, M., Li, Q., Xie, G., Ore, B. M., Qiao, S., Spencer, M. D., Zeisel, S. H., Zhou, Z., Zhao, A., Jia, W., *Metabolomics*, 2013, 9, 818-827.

[28] He, L., Prodhan, M. A. I., Yuan, F., Yin, X., Lorkiewicz, P. K., Wei, X., Feng, W., McClain, C., Zhang, X., *J Chromatogr B Analyt Technol Biomed Life Sci.*, 2018, 1092, 359-367.

[29] Li, Z., Yi, C. X., Katiraei, S., Kooijman, S., Zhou, E., Chung, C. K., Gao, Y., van den Heuvel, J. K., Meijer, O. C., Berbée, J. F. P., Heijink, M., Giera, M., Willems van Dijk, K., Groen, A. K., Rensen, P. C. N., Wang, Y., *Gut,* 2018, 67, 1269-1279.

[30] Tomcik, K., Ibarra, R. A., Sadhukhan, S., Han, Y., Tochtrop, G. P., Zhang, G. F., *Anal Biochem.*, 2011, 410, 110-7.

[31] Zhang, S., Wang, H., Zhu, M., *Talanta*, 2019, 196, 249-254.

[32] Lotti, C., Rubert, J., Fava, F., Tuohy, K., Mattivi, F., Vrhovsek, U., *Anal Bioanal Chem.*, 2017, 409, 5555-5567.

[33] Hsu, Y. L., Chen, C. C., Lin, Y. T., Wu, W. K., Chang, L. C., Lai, C. H., Wu, M. S., Kuo, C. H., *J Proteome Res.*, 2019, 18, 1948-1957.

[34] Han, X., Guo, J., You, Y., Yin, M., Ren, C., Zhan, J., Huang, W., *J. Chromatogr. B,* 2018, 1099, 73-82.

[35] Fiori, J., Turroni, S., Candela, M., Brigidi, P., Gotti, R., *Talanta*, 2018, 189, 573-578.

[36] De Baere, S., Eeckhaut, V., Steppe, M., De Maesschalck, C., De Backer, P., Van Immerseel, F., Croubels, S., *J Pharm Biomed Anal.*, 2013, 80, 107-15.

[37] Gardana, C., Del Bo', C., Simonetti, P., *J Pharm Biomed Anal.*, 2017, 141, 46-51.

[38] Han, J., Lin, K., Sequeira, C., Borchers, C. H., *Anal Chim Acta.,* 2015, 854, 86-94.

[39] Chan, J. C., Kioh, D. Y., Yap, G. C., Lee, B. W., Chan, E. C., *J Pharm Biomed Anal.*, 2017, 138, 43-53.

[40] Ma, S. R., Tong, Q., Zhao, Z. X., Cong, L., Yu, J., Fu, J., Han, P., Pan, L., Gu, R., Peng, R., Zhang, Z., Wang, Y., Jiang, J., *Anal Bioanal Chem.,* 2019, 411, 3191–3207.

[41] Nagatomo, R., Okada, Y., Ichimura, M., Tsuneyama, K., Inoue, K., *Anal Sci.*, 2018, 34, 1031-1036.

[42] Zeng, M., Cao, H., *J Chromatogr B Analyt Technol Biomed Life Sci.*, 2018, 1083, 137-145.

[43] Song, H. E., Lee, H. Y., Kim, S. J., Back, S. H., Yoo, H. J., *Metabolites,* 2019, 9, 173

[44] Marques, L. A., Cazarin, C. B. B., Bicas, J., Marostica Junior, M. R., Carrilho, E., Bogusz Junior, S., *J. Braz. Chem. Soc.*, 2019, 30, 1326-1333

[45] Hodek, O., Krizek, T., *Anal. Methods*, 2019, 11, 4575

[46] Lemay, J. A., Yamamoto, M., Kroezen, Z., Shanmuganathan, M., Ly, R., Hart, L., Pai, N., Britz-McKibbin, P., *J Pharm Biomed Anal.*, 2021, 192, 113658.

[47] Macka, M., Haddad, P. R., *Electrophoresis*, 1997, 18, 2482–2501.

[48] Shamsi, S. A., in *Encyclopedia of Analytical Chemistry* (eds R.A. Meyers and I.M. Warner), 2006.

[49]   Ackermans, M. T., Everaerts, F. M., Beckers, J. L., *J. Chromatogr. A*, 1991, 549, 345–355.

[50]   Jones, W. R., Jandik, P., in *Handbook of Capillary Electrophoresis*, ed. J.P. Landers, 216–217.

[51]   Weston, A., Brown, P. R., Jandik, P., Heckenberg, A. L., Jones, W. R., *J. Chromatogr. A*, 1992, 608, 395–402.

Chapter 2

[1]   Hoeven, R. S., Steffens, J. C., *Plant Physiol.* 2000, *122*, 275–282.

[2]   Besten, G., Eunen, K., Groen, A. K., Venema, K., Reijngoud, D., Bakker, B. M., *J Lipid Res.* 2013, *54*, 2325–2340.

[3]   Primec, M., Micetic-Turk, D., Langerholc, T., *Anal Biochem.* 2017, *526*, 9-21.

[4]   Igarashi, H., Ohno, K., Matsuki, N., Fujiwara-Igarashi, A., Kanemto, H., Fukushima, H., Uchida, K., Tsujimoto, H., *J. Vet. Med. Sci.* 2017, *79*, 1727–1734.

[5]   Zhao, X., Jiang, Z., Yang, F., Wang, Yan, Gao, X., Wang, Yuefei, Chai, X., Pan, G., Zhu, Y., *PLoS One* 2016, *11*, e0167032.

[6]   Chang, Y., Chen, Y., Zhou, Q., Wang, C., Chen, L., Di, W., Zhang, Y., *Clin Sci (Lond)* 2020, *134*, 289–302.

[7]   Lemarie, F., Beuchamp, E., Legrand, P., Rioux, V., *Biochimie* 2016, *120*, 40-48.

[8]   Fiori, J., Turroni, S., Candela, M., Gotti, R., *J. Pharm. Biomed. Anal.* 2020, *177*, 112867.

[9]   Marques, L. A., Cazarin, C. B. B., Bicas, J., Marostica Junior, M. R., Carrilho, E., Bogusz Junior, S., *J. Braz. Chem. Soc.* 2019, *30*, 1326-1333.

[10]   Hodek, O., Krizek, T., *Anal. Methods* 2019, *11*, 4575.

[11]   Turkia, H, Siren, H., Pitkanen, J. P., Wiebe, M., Penttila, M., *J. Chromatogr. A* 2010, *1217*, 1537–1542.

[12]   Rovio, S., Kalliola, A., Siren, H., Tamminen, T., *J. Chromatogr. A* 2010, *1217*, 1407–1413.

[13]   Fung, Y., S., Tung, H. S., *Electrophoresis* 2001, *22*, 2242– 2250

[14]   Rivasseau, C., Boisson, A. M., Mongerald, G., Couram, G., Bastien, O., Bligny, R., *J. Chromatogr. A* 2006, *1229*, 283– 290.

[15]   Hagberg, J., Dahlen, J., Karlsson, S., Allard, B., *Int. J. Environ. Anal. Chem.* 2000, *78*, 385–396.

[16]   Gao, S., Rudolph, J., *J. Chromatogr. Sci.* 2004, *42*, 323–328.

[17]   Lemay, J. A., Yamamoto, M., Kroezen, Z., Shanmuganathan, M., Ly, R., Hart, L., Pai, N., Britz-McKibbin, P., *J Pharm Biomed Anal.*, 2021, 192, 113658.

[18]   Song, H. E., Lee, H. Y., Kim, S. J., Back, S. H., Yoo, H. J., *Metabolites* 2019, *9*, 173.

[19]   Haddadian F., Shamsi, S.A., Warner, I.M., *J. Chromatogr. Sci.* 1999, *37*, 103– 107.

[20]   Bannore, Y. C., Chenault, K. D., Melouk, H. A., Rassi, Z. E., *J Sep Sci.* 2008, *31*, 2667–76.

[21]   Tabaumi, S., Endo, S., Akagawa, H., Itabashi, Y., *Bunseki Kagaku* 2003, *52*, 847–850.

[22]   Shamsi, S. A., Danielson, N. D., *Anal. Chem.* 1995, *67*,1842-1852.

[23]   Schaeper, J. P., Shamsi, S. A., Danielson, N. D., *J. Cap. Electrophoresis.* 1996, *3*, 215-221.

[24]   Shamsi, S. A., Weathers, R. M., Danielson, N. D., *J. Chromatogr A.* 1996, *737*, 315-324.

[25]   Gas, B., Hruska, V., Dittmann, M., Bek, F., *J. Sep Science.* 2007, 30, 1435-1445.

[26]   Hayakawa, K., Nakamura, S., Inaki, K., Miyazaki, M., *Anal. Sci.* 1989, 5, 691-695.

[27]   Hashidzume, A., Takashima, Y., Yamaguchi, H., Harada, A., *Compr. Supramol. Chem. II* 2017, 269–316.

[28]   Golubenko, A.M., Nikonorov, V.V., Nikitina, T.G. *J Anal Chem* 2012, *67*, 778–782.

[29]   Shamsi, S. A., Danielson, N. D., *Anal Chem.* 1994, *66*, 3757 – 3764.

[30]   Mantel, M., Stiller, M., *Anal. Chem.* 1976, *48*, 712–714.

[31]   Windholz, M., "The Merck Index: an encyclopedia of chemicals, drugs, and biologicals" Rahway, New Jersey: Merck & Co., Inc. 1976, 21.

[32]   Copper, C. L., *J. Chem. Educ.* 1998, *75*, 343-346.

[33]   Suess, G. J., Kasiah, J., Anthony, B., Williams, B., Chassaing, B. F., Frantz, K. J., *AbstViewer/Itinerary Planner, Soc for Neurosci.* Chicago, 2019.

[34]   Kiraly, D. D., Walker, D. M., Calipari, E. S., Labonte, B., Issler, O., Pena, C. J., Ribeiro, E. A., Russo, S. J., Nestler, E. J., *Scientific Reports* 2016 *6* (1).

Chapter 3

[1]   Shaidullov, I. F., Sorokina, D. M., Sitdikov, F. G., Hermann, A., Abdulkhakov, S. R., Sitdikova, G. F., *BMC Gastroenterol.* 2021, *21*, 37.

[2]   Magzal, F., Even, C., Haimov, I., Agmon, M., Asraf, K., Shochat, T., Tamir, S., *Sci Rep.* 2021, *11,* 4052.

[3]   Calderón-Pérez, L., Gosalbes, M.J., Yuste, S., Valls, R. M., Pedret, A., Llaurado, E., Jimenez-Hernandez, N., Artacho, A., Pla-Paga, L., Companys, J., Ludwid, I., Romero, M., Rubio, L., Sola, R., *Sci Rep.* 2020, *10,* 6436.

[4]   Jiang, D., Guo, S., Kang, A., Ju, Y., Li, J., Yu, S., Bao, B., Cao, Y., Tang, Y., Zhang, L., Yao, W., *Pharm Biol.* 2020, *58* (1), 367-373.

[5]   Shah, S., Fillier, T., Pham, T. H., Thomas, R., Cheema, S. K., *Nutrients.* 2021, *13* (3), 892.

[6]   Byrne, C. S., Chambers, E. S., Morrison, D. J., Frost, G., *Int J Obes (Lond).* 2015, *39* (9), 1331-1338.

[7]   Silva, Y. P., Bernardi, A., Frozza, R. L., *Front. Endocrinol.* 2020, *11*, 25.

[8]   Dalile, B., Van Oudenhove, L., Vervliet, B., Verbeke, K.,. *Nat. Rev. Gastroenterol. Hepatol.* 2019, *16*, 461–478.

[9]   Möhle, L., Mattei, D., Heimesaat, M. M., Bereswill, S., Fischer, A., Alutis, M., French, T., Hambardzumyan, D., Matzinger, P., Dunay, I. R., Wolf, S. A., *Cell Rep.* 2016, *15*, 1945–56.

[10]   Holota, Y., Dovbynchuk, T., Kaji, I., Vareniuk, I., Dzyubenko, N., Chervinska, T., Zakordonets, L., Stetska, V., Ostapchenko, L., Serhiychuk, T., Tolstanova, G., *PLoS ONE* 2019, *14* (8): e0220642.

[11]   Stanisavljević, S., Cepić, A., Bojić, S., Veljović, K., Mihajlović, S., Đedović, N., Jevtić, B., Momcilović, M., Lazarević, M., Stoiković, M. M., Miljković, Đ., Golić, N., *Sci Rep.* 2019, *9*, 1–13.

[12] Mårild K, Ye W, Lebwohl B, Green PH, Blaser MJ, Card T, *BMC Gastroenterol.* 2013; *13*:109.

[13] Horton DB, Scott FI, Haynes K, Putt ME, Rose CD, Lewis JD, *Pediatrics.* 2015; *136*(2):e333–43.

[14] Scott FI, Horton DB, Mamtani R, Haynes K, Goldberg DS, Lee DY, *Gastroenterology.* 2016; *151*(1):120–129.e5.

[15] Hviid A, Svanstro¨m H, Frisch M. *Gut.* 2011; *60*(1):49–54.

[16] Shaw SY, Blanchard JF, Bernstein CN. *Am J Gastroenterol.* 2011; *106*(12):2133–42.

[17] Chivero, E. T., Ahmad, R., Thangaraj, A., Periyasamy, P., Kumar, B., Kroeger, E., Feng, D., Guo, M., Roy, S., Dhawan, P.,Singh, A. B., Buch, S., *Sci Rep* 2019, *9*, 12187.

[18] Gibbons, T. E., Sayed, K., Fuchs, G. J., *World J Pediatr. 2009, 5*, 149–151.

[19] Zhao, X., Jiang, Z., Yang, F., Wang, Yan, Gao, X., Wang, Yuefei, Chai, X., Pan, G., Zhu, Y., *PLoS One* 2016, *11*, e0167032.

[20] Hsu, Y. L., Chen, C. C., Lin, Y. T., Wu, W. K., Chang, L. C., Lai, C. H., Wu, M. S., Kuo, C. H., *J Proteome Res.*, 2019, 18, 1948-1957.

[21] Song, H. E., Lee, H. Y., Kim, S. J., Back, S. H., Yoo, H. J., *Metabolites* 2019, *9*, 173.

[22] Ma, S. R., Tong, Q., Zhao, Z. X., Cong, L., Yu, J., Fu, J., Han, P., Pan, L., Gu, R., Peng, R., Zhang, Z., Wang, Y., Jiang, J., *Anal Bioanal Chem.,* 2019, 411, 3191–3207.

[23] Marques, L. A., Cazarin, C. B. B., Bicas, J., Marostica Junior, M. R., Carrilho, E., Bogusz Junior, S., *J. Braz. Chem. Soc.*, 2019, *30*, 1326-1333

[24] Hodek, O., Krizek, T., *Anal. Methods*, 2019, *11*, 4575

[25] Lemay, J. A., Yamamoto, M., Kroezen, Z., Shanmuganathan, M., Ly, R., Hart, L., Pai, N., Britz-McKibbin, P., *J Pharm Biomed Anal.*, 2021, *192*, 113658.

[26] Hewavitharana, A. K., Abu Kassim, N. S., Shaw, P. N., *J Chromatogr A.* 2018, *1553,* 101-107.

[27] FDA, *Analytical Procedures and Methods Validation for Drugs and Biologics, Guidance for Industry* (CDER, July 2015).

[28] Tao, J., Duan, J., Jiang, S., Guo, J., Qian, Y., Qian, D., *J. Chromatogr. B* 2016, *1029–1030*, 88-94.

[29] Jaochico, A., Sangaraju, D., Shahidi-Latham, S. K., *Bioanalysis.* 2019, *11* (8), 741-753.

[30] Panuwet, P., Hunter Jr., R. E., D'Souza, P. E., Chen, X., Radford, S. A., Cohen, J. R., Marder, M. E., Kartavenka, K., Ryan, P. B., Barr, D. B., *Crit Rev Anal Chem.* 2016, *46* (2), 93-105.

[31] Nagpal, R., Wang, S., Solberg, W. L. C., Seshie, O., Chung, S. T., Shively, C. A., Register, T. C., Craft, S., McClain, D. A., Yadav, H., *Front. Microbiol.*, 2018 *9*:2897

[32] Zhao, X., Jiang, Z., Yang, F., Wang, Y., Gao, X., Wang, Y., Chai, X., Pan, G., Zhu, Y., *PLoS ONE*, 2016, *11*, e0167032.

[33] Hoverstad, T., Carlstedt-Duke, B., Lingaas, E., Midtvedt, T., Norin, K. E., Saxerholt, H., Steinbakk, M., *Scand J Gastroenterol.* 1986, *21*, 621-626.

[34]   Weitkunat, K., Schumann, S., Petzke, K. J., Blaut, M., Loh, G., Klaus, S., *J Nutr Biochem*. 2015, *26*, 929-37.